lectin microarray analysis of these cells and their parental MRC-5 cells. The iPS cell lines were clearly distinguishable from their parental cell MRC-5 (Fig. 4A,B). We then performed the lectin microarray analysis on iPS lines and their differentiated forms. All differentiated ES cells (EB; EB_H8, EB_H9 and EB_H3) were categorized into the group including MRC-5 parental cells, and undifferentiated iPS cells were categorized into the same group with hES cells (Fig. 4B). These results suggest that glycomic analysis using lectin microarray presents a specific lectin profile for pluripotency.

Generation of discriminant functions for pluripotency of human stem cells

To define pluripotency of human ES and iPS cells, we constructed seven formulas with the combination of the selected three lectins, MAL, PHA(L) and EEL (Table 1), using the lectin microarray data of 3 hES cells and 3 differentiated cells (EB) as a training set (Table S1 in Supporting Information). The criterion for classifying undifferentiated and differentiated from of pluripotent cells is as follows: if *Score value* is >0 or equal to 0, cells are categorized into 'pluripotent' cell population, and if *Score value* is <0, cells are categorized into 'nonpluripotent/differentiated' cell population. To evaluate the accuracy of these functions, we used the lectin microarray data of MRC-5-derived iPS cells and MRC-5 parental cells as a test set (Table 2A and Table S2 in Supporting Information). Linear discriminant function with the combination of PHA(L) and EEL (Formula 6: $F = -1.75 \times PHA(L) + 1.28 \times EEL + 1.92$) shows the highest accuracy (100%) of determination of pluripotency, followed by that of MAL and EEL (Formula 5: $F = -2.45 \times MAL + 1.23 \times EEL + 1.45$) (97%), whereas the discriminant function with the combination of three lectins (Formula 7: $F = -2.98 \times MAL + 0.75 \times PHA(L) + 1.44 \times EEL + 0.70$) and MAL and PHA(L) (Formula 4: $F = -2.81 \times MAL + 0.03 \times PHA(L) + 2.29$) shows 86.6% and 55.2%, respectively. Determination with single lectins shows 94.0% (Formula 2: $F = -2.38 \times PHA(L) + 3.46$), 55.2% (Formula 1: $F = -2.78 \times MAL + 2.32$) and 89.6% (Formula 3: $F = 2.59 \times EEL + 1.25$) accuracy. We then analyzed lectin profiles on iPS cells derived from amniotic mesoderm (Nagata *et al.* 2009) (Table 2B, Tables S3 and S5 in Supporting Information). Formula 6 with PHA(L) and EEL as variants generated the highest accuracy (100.0%) among the formulas generated. These results suggest that two lectins, EEL and PHA(L), are most suitable to determine pluripotency of stem cells. To investigate if scores calculated from each formula are correlated with 'pluripotency', we performed RT-PCR analysis of stem cell-specific genes. Positive correlations were observed between the scores and expression of the *OCT4/3* and *NANOG* genes (Fig. 4C).

Table 1 Discriminant functions

No.	Combination of lectins	Formula
1	MAL	$F = -2.78 \times MAL + 2.32$
2	PHA(L)	$F = -2.38 \times PHA(L) + 3.46$
3	EEL	$F = 2.59 \times EEL + 1.25$
4	MAL, PHA(L)	$F = -2.81 \times MAL + 0.03 \times PHA(L) + 2.29$
5	MAL, EEL	$F = -2.45 \times MAL + 1.23 \times EEL + 1.45$
6	PHA(L), EEL	$F = -1.75 \times PHA(L) + 1.28 \times EEL + 1.92$
7	MAL, PHA(L), EEL	$F = -2.98 \times MAL + 0.75 \times PHA(L) + 1.44 \times EEL + 0.70$

Table 2 Evaluation of discriminant functions

Formula number	Sensitivity (%)	Specificity (%)	Accuracy (%)
(A) MRC-derived iPS cells			
1	50	100	55.2
2	93.3	100	94
3	93.3	57.1	89.6
4	50	100	55.2
5	96.7	100	97
6	100	100	100
7	85	100	86.6
(B) AM-derived iPS cells			
1	0	100	16.7
2	10	100	25
3	100	50	91.7
4	0	100	16.7
5	60	100	66.7
6	100	100	100
7	70	100	75

$$\text{Sensitivity} = \frac{\text{Number of true positives}}{\text{Number of true positives} + \text{number of false negatives}}$$

$$\text{Specificity} = \frac{\text{Number of true negatives}}{\text{Number of true negatives} + \text{Number of false positives}}$$

$$\text{Accuracy} = \frac{\text{Number of true positives} + \text{Number of true negatives}}{\text{Number of positives} + \text{Number of negatives}}.$$

Discussion

The goal of this study was to distinguish oligosaccharide structures that are increased in pluripotent and

multipotent cell types. Categorization using lectin probes enabled us to distinguish between different stem cell potencies or to discriminate between undifferentiated and differentiated forms. These results could lead to the use of lectin profiling as a tool for the better understanding of cell identity. To date, global glycan profiles have been preferentially analyzed by mass spectrometry (Satomaa *et al.* 2009; Wollscheid *et al.* 2009). Specifically, high- resolution mass spectrometry is the primary technique for characterizing the structures of individual glycans in most glycomic studies (Satomaa *et al.* 2009; Alvarez-Manilla *et al.* 2010). Mass spectrometry can also be employed to define sites of attachment of glycans to the underlying protein scaffold. A major benefit of mass spectrometry is the detailed information it provides regarding the structure of a glycan. A drawback, however, is its relatively low throughput and the need for different experimental protocols for each glycan subtype. In contrast, lectin microarray can be employed to interrogate the glycome with much higher throughput and provide global information about the types of glycan epitopes that are present in the sample (Kuno *et al.* 2005; Yue & Haab 2009; Porter *et al.* 2010). The high-throughput platform as well as satisfactory sensitivity allows rapid comparison of multiple glycomes in search of global changes that might motivate further mass spectrometry studies.

Glycan-based quality control for cell therapy—Defining the states of pluripotent stem cells

In cell-based therapy, lectin microarray is a practical tool for the quality control of stem cell products. Flow cytometric analysis and immunocytochemical analysis with single probes have been used in this regard, but the lectin microarray technique with multiple probes provides an opportunity to address this issue in a simple, inexpensive and fast manner (Katrlik *et al.* 2010). Cell identity needs to be validated after each step of cell processing, i.e., isolation, *in vitro* propagation, harvesting and transfer because cells may be modified or changed after either of these steps and should thus be monitored by the most trustworthy method. Human ES and iPS cells for potential use as donor cells in cell-based therapy need to be validated for maintenance of the 'undifferentiated' state during *in vitro* propagation and while stored in master and working cell banks (Wobus & Boheler 2005; Yamanaka 2009). Lectin microarray techniques for precise monitoring of the undifferentiated or differentiated state are indeed sensitive and only a small number of cells (1×10^3) are sufficient to obtain reproducible results. This feature of the technology, to define diverse cell identities, also leads to high-throughput screening for drug discovery and toxicology and safety testing.

Glycan profile to determine cell identity

Hematopoietic stem cells were originally defined by GlcNAc-specific wheat germ agglutinin (WGA), one of the most common plant lectins (Spangrude *et al.* 1988), and human and murine endothelial cells were defined by another lectin, α1-2Fuc-specific *Ulex europaeus* agglutinin I (UEA-I) (Jackson *et al.* 1990). Neural stem cells were also defined by the glycolipid antigen LeX/SSEA-1 (Capela & Temple 2002). Furthermore, human ES and iPS cells have been previously evaluated by the presence of carbohydrate markers. The International Stem Cell Initiative characterized 59 human ES cell lines from 17 laboratories worldwide. Human ES cell lines are characterized by carbohydrate markers such as the glycolipid antigens SSEA3 and SSEA4, and the keratan sulfate antigens TRA-1-60, TRA-1-81, GCTM2 and GCT343 as well as the protein antigens (Adewumi *et al.* 2007; Wright & Andrews 2009). In addition to detection of carbohydrate markers by lectins and antibody probes, comprehensive glycan analysis serves as another method to detect and define cell identities. In this study, we found the pluripotent stem cells have the specific glycan structure, Galα1-3Gal, recognized by EEL (Fig. S1 in Supporting Information). Their major specific N-glycosylation feature in hES cells is complex fucosylation (Satomaa *et al.* 2009), whereas PHA(E) ligands are signs of hES cell differentiation (Venable *et al.* 2005; Wearne *et al.* 2006). This study suggests that glycan profiling by lectin microarray is more sensitive, compared with any other analysis. Further analysis of stem cell glycan may also lead to establishing new glycan structures as stem cell markers in addition to the commonly used SSEA and TRA glycan structures.

Glycans function as ligands for specific glycan receptors and modulate the activity of their carrier proteins and lipids (Imperiali & O'Connor 1999; Zanetta & Vergoten 2003). More than half of all proteins in a human cell are glycosylated. Consequently, a global change in protein-linked glycan biosynthesis can simultaneously modulate the properties of multiple proteins. It is likely that drastic changes during differentiation of human stem cells have major influences on a number of cellular signaling cascades and affect biological processes within the cells (Xu *et al.* 2005; Sasaki *et al.*

2008). Thus, glycan profiling can be useful for validation of cell identity (Satomaa *et al.* 2009). Categorization of stem cells by lectin microarray analysis can become another fundamental method in addition to immunocytochemistry and flow cytometric analysis. Microarray technologies currently enhance our understanding of gene expression, genomic stability and epigenetics, are commonly used in research laboratories and clinics today, and will likely play important roles in advancing stem cell research. In the future, analysis of stem cell glycan structure may be useful for establishing new markers beyond the lectin markers that already play a major role in the rapidly evolving world of stem cell biology.

Experimental procedures

Cells and cell culture

9-15c (uncommitted stem cells), H-1/A (preadipocytes), KUM5 (chondroblasts) and KUSA-A1 (osteoblasts) are available through cell banks (JHSF cell bank: http://www.jhsf.or.jp/English/index_gc.html; RIKEN cell bank: http://www.brc.riken.go.jp/lab/cell/english/). 9-15c (Yamada *et al.* 2007), H-1/A (Umezawa *et al.* 1991), KUM5 (Sugiki *et al.* 2007) and KUSA-A1 cells (Umezawa *et al.* 1992) were cultured using methods described previously. The cells were maintained in POWEREDBY10 medium (MED SHIROTORI CO., Ltd, Tokyo, Japan) or Iscove's modified Dulbecco's medium (IMDM) supplemented with 20% fetal bovine serum and penicillin (100 μg/mL)/streptomycin (100 μg/mL)/amphotericin B (250 ng/mL) at 33 °C with 5% CO_2. Human mesenchymal cells were maintained in DMEM (Sigma, St. Louis, MO) supplemented with 100 μg/mL penicillin, 100 IU/mL streptomycin and 10% fetal calf serum at 37 °C in a CO_2 incubator. Human embryonal carcinoma cell line NCR-G3, from a testicular tumor, was cultured in G031101 medium (Med Shirotori, Tokyo, Japan) as previously described (Maruyama *et al.* 1996; Umezawa *et al.* 1996). Human iPS cells were cultured in Valuegen medium (Med Shirotori, Tokyo, Japan) (Makino *et al.* 2009; Nagata *et al.* 2009).

Extraction of membrane fractions and lectin microarray analysis

Cells ($0.1–1 \times 10^6$) were washed with PBS and collected with a cell scraper. Cell pellets of hES-3, -8, and -9 cells (Osafune *et al.* 2008) were kindly obtained from Dr Douglas Melton (Harvard University). Cell membrane fractions were extracted from the cell pellets using a CelLytic MEM Protein Extraction kit (Sigma, St Louis, MO, USA). Lectin microarray analysis was performed as previously described (Kuno *et al.* 2005, 2008). Briefly, a small aliquot of protein fraction (200 ng) was labeled with Cy3-succinimidyl ester (designated as Cy3-labeled glycoprotein). The lectin chip with 43 lectins (Kuno *et al.* 2005) for mouse cells or LecChip™ with 45 lectins (GP Bio-Sciences, Kanagawa, Japan) for human cells was incubated with the Cy3-labeled glycoprotein solution (100 μL) at a concentration of 0.25 and 0.5 μg/mL in probing buffer (TBS containing 0.05% Triton X-100) at 4 °C until binding reached equilibrium. Lectins are well known as glycan recognizers and are classified into several categories, for instance, fucose, sialic acid, asialo-form, agalacto-form, high mannose, O-glycan and branching structure recognizers (Fig. S1 in Supporting Information). We calculated the net intensity value for each spot by subtracting a background value from signal intensity and then averaged the signal net intensity values of three spots. Lectin microarray data on each cell type were processed by the microarray system using a max-normalization procedure after a gain-merging process (Kuno *et al.* 2008).

Hierarchical clustering analysis and principal component analysis

To analyze the lectin microarray data, we used agglomerative hierarchical clustering and principal component analysis (PCA) (Sharov *et al.* 2005). The hierarchical clustering techniques classify data by similarity and their results are represented by dendrograms. PCA is a multivariate analysis technique that finds major patterns in data variability.

Discriminant analysis of pluripotency in human pluripotent stem cells

Coefficients and constants of each formula were defined, using the lda function in the MASS library of the statistical package R [http://www.r-project.org/, (Venables & Ripley 2002), (Ripley 1996)].

Acknowledgement

We express our sincere thanks to C. Ketcham for reviewing the manuscript, M. Yamada for fruitful discussion and critical reading of the manuscript, Y. Takahashi for providing expert technical assistance and to K. Saito and Y. Kajiyama for secretarial work. This work was supported in part by a grant for New Energy and Industrial Technology Development Organization (NEDO) in Japan; Health and Labour Sciences Research Grants; and grants from the Ministry of Education, Culture, Sports, Science and Technology (MEXT) of Japan.

References

Adewumi, O., Aflatoonian, B., Ahrlund-Richter, L., *et al.* (2007) Characterization of human embryonic stem cell lines by the international stem cell initiative. *Nat. Biotechnol.* **25**, 803–816.

Alvarez-Manilla, G., Warren, N.L., Atwood, J. III, Orlando, R., Dalton, S. & Pierce, M. (2010) Glycoproteomic analysis of embryonic stem cells: identification of potential glycobiomarkers using lectin affinity chromatography of glycopeptides. *J. Proteome Res.* **9**, 2062–2075.

Angeloni, S., Ridet, J.L., Kusy, N., Gao, H., Crevoisier, F., Guinchard, S., Kochhar, S., Sigrist, H. & Sprenger, N. (2005) Glycoprofiling with micro-arrays of glycoconjugates and lectins. *Glycobiology* **15**, 31–41.

Aoi, T., Yae, K., Nakagawa, M., Ichisaka, T., Okita, K., Takahashi, K., Chiba, T. & Yamanaka, S. (2008) Generation of pluripotent stem cells from adult mouse liver and stomach cells. *Science* **321**, 699–702.

Budnik, B.A., Lee, R.S. & Steen, J.A. (2006) Global methods for protein glycosylation analysis by mass spectrometry. *Biochim. Biophys. Acta* **1764**, 1870–1880.

Capela, A. & Temple, S. (2002) LeX/ssea-1 is expressed by adult mouse CNS stem cells, identifying them as nonependymal. *Neuron* **35**, 865–875.

Ebe, Y., Kuno, A., Uchiyama, N., Koseki-Kuno, S., Yamada, M., Sato, T., Narimatsu, H. & Hirabayashi, J. (2006) Application of lectin microarray to crude samples: differential glycan profiling of lec mutants. *J. Biochem.* **139**, 323–327.

Imperiali, B. & O'Connor, S.E. (1999) Effect of N-linked glycosylation on glycopeptide and glycoprotein structure. *Curr. Opin. Chem. Biol.* **3**, 643–649.

Jackson, C.J., Garbett, P.K., Nissen, B. & Schrieber, L. (1990) Binding of human endothelium to Ulex europaeus I-coated Dynabeads: application to the isolation of microvascular endothelium. *J. Cell Sci.* **96** (Pt 2), 257–262.

Kaichi, S., Hasegawa, K., Takaya, T., Yokoo, N., Mima, T., Kawamura, T., Morimoto, T., Ono, K., Baba, S., Doi, H., Yamanaka, S., Nakahata, T. & Heike, T. (2010) Cell line-dependent differentiation of induced pluripotent stem cells into cardiomyocytes in mice. *Cardiovasc. Res.* **88**, 314–323.

Katrlik, J., Svitel, J., Gemeiner, P., Kozar, T. & Tkac, J. (2010) Glycan and lectin microarrays for glycomics and medicinal applications. *Med. Res. Rev.* **30**, 394–418.

Kuno, A., Itakura, Y., Toyoda, M., Takahashi, Y., Yamada, Y., Umezawa, A. & Hirabayashi, J. (2008) Development of a data-mining system for differential profiling of cell glycoproteins based on lectin microarray. *J. Proteomics Bioinform.* **1**, 068–072.

Kuno, A., Uchiyama, N., Koseki-Kuno, S., Ebe, Y., Takashima, S., Yamada, M. & Hirabayashi, J. (2005) Evanescent-field fluorescence-assisted lectin microarray: a new strategy for glycan profiling. *Nat. Methods* **2**, 851–856.

Lee, J.H., Schell, M.J. & Roetzheim, R. (2009) Analysis of group randomized trials with multiple binary endpoints and small number of groups. *PLoS ONE* **4**, e7265.

Makino, H., Toyoda, M., Matsumoto, K., *et al.* (2009) Mesenchymal to embryonic incomplete transition of human cells by chimeric OCT4/3 (POU5F1) with physiological co-activator EWS. *Exp. Cell Res.* **315**, 2727–2740.

Maruyama, T., Umezawa, A., Kusakari, S., Kikuchi, H., Nozaki, M. & Hata, J. (1996) Heat shock induces differentiation of human embryonal carcinoma cells into trophectoderm lineages. *Exp. Cell Res.* **224**, 123–127.

Matsumoto, S., Shibuya, I., Kusakari, S., Segawa, K., Uyama, T., Shimada, A. & Umezawa, A. (2005) Membranous osteogenesis system modeled with KUSA-A1 mature osteoblasts. *Biochim. Biophys. Acta* **1725**, 57–63.

Nagata, S., Toyoda, M., Yamaguchi, S., Hirano, K., Makino, H., Nishino, K., Miyagawa, Y., Okita, H., Kiyokawa, N., Nakagawa, M., Yamanaka, S., Akutsu, H., Umezawa, A. & Tada, T. (2009) Efficient reprogramming of human and mouse primary extra-embryonic cells to pluripotent stem cells. *Genes Cells* **14**, 1395–1404.

Osafune, K., Caron, L., Borowiak, M., Martinez, R.J., Fitz-Gerald, C.S., Sato, Y., Cowan, C.A., Chien, K.R. & Melton, D.A. (2008) Marked differences in differentiation propensity among human embryonic stem cell lines. *Nat. Biotechnol.* **26**, 313–315.

Pilobello, K.T., Krishnamoorthy, L., Slawek, D. & Mahal, L.K. (2005) Development of a lectin microarray for the rapid analysis of protein glycopatterns. *Chembiochem* **6**, 985–989.

Porter, A., Yue, T., Heeringa, L., Day, S., Suh, E. & Haab, B.B. (2010) A motif-based analysis of glycan array data to determine the specificities of glycan-binding proteins. *Glycobiology* **20**, 369–380.

Ripley, B.D. (1996) *Pattern Recognition and Neural Networks.* Cambridge: Cambridge University Press.

Sasaki, N., Okishio, K., Ui-Tei, K., Saigo, K., Kinoshita-Toyoda, A., Toyoda, H., Nishimura, T., Suda, Y., Hayasaka, M., Hanaoka, K., Hitoshi, S., Ikenaka, K. & Nishihara, S. (2008) Heparan sulfate regulates self-renewal and pluripotency of embryonic stem cells. *J. Biol. Chem.* **283**, 3594–3606.

Satomaa, T., Heiskanen, A., Mikkola, M., *et al.* (2009) The N-glycome of human embryonic stem cells. *BMC Cell Biol.* **10**, 42.

Sharon, N. & Lis, H. (2004) History of lectins: from hemagglutinins to biological recognition molecules. *Glycobiology* **14**, 53R–62R.

Sharov, A.A., Dudekula, D.B. & Ko, M.S. (2005) A web-based tool for principal component and significance analysis of microarray data. *Bioinformatics (Oxford, England)* **21**, 2548–2549.

Spangrude, G.J., Heimfeld, S. & Weissman, I.L. (1988) Purification and characterization of mouse hematopoietic stem cells. *Science* **241**, 58–62.

Sugiki, T., Uyama, T., Toyoda, M., Morioka, H., Kume, S., Miyado, K., Matsumoto, K., Saito, H., Tsumaki, N., Takahashi, Y., Toyama, Y. & Umezawa, A. (2007) Hyaline cartilage formation and enchondral ossification modeled with KUM5 and OP9 chondroblasts. *J. Cell. Biochem.* **100**, 1240–1254.

Takahashi, K., Tanabe, K., Ohnuki, M., Narita, M., Ichisaka, T., Tomoda, K. & Yamanaka, S. (2007) Induction of pluripotent stem cells from adult human fibroblasts by defined factors. *Cell* **131**, 861–872.

Tateno, H., Uchiyama, N., Kuno, A., Togayachi, A., Sato, T., Narimatsu, H. & Hirabayashi, J. (2007) A novel strategy for mammalian cell surface glycome profiling using lectin microarray. *Glycobiology* **17**, 1138–1146.

Umezawa, A., Maruyama, T., Inazawa, J., Imai, S., Takano, T. & Hata, J. (1996) Induction of mcl1/EAT, Bcl-2 related gene, by retinoic acid or heat shock in the human embryonal carcinoma cells, NCR-G3. *Cell Struct. Funct.* **21**, 143–150.

Umezawa, A., Maruyama, T., Segawa, K., Shadduck, R.K., Waheed, A. & Hata, J. (1992) Multipotent marrow stromal cell line is able to induce hematopoiesis *in vivo*. *J. Cell. Physiol.* **151**, 197–205.

Umezawa, A., Tachibana, K., Harigaya, K., Kusakari, S., Kato, S., Watanabe, Y. & Takano, T. (1991) Colony-stimulating factor 1 expression is down-regulated during the adipocyte differentiation of H-1/A marrow stromal cells and induced by cachectin/tumor necrosis factor. *Mol. Cell. Biol.* **11**, 920–927.

Varki, A. (1993) Biological roles of oligosaccharides: all of the theories are correct. *Glycobiology* **3**, 97–130.

Venable, A., Mitalipova, M., Lyons, I., Jones, K., Shin, S., Pierce, M. & Stice, S. (2005) Lectin binding profiles of SSEA-4 enriched, pluripotent human embryonic stem cell surfaces. *BMC Dev. Biol.* **5**, 15.

Venables, W.N. & Ripley, B.D. (2002) *Modern Applied Statistics with S*, 4th edn. New York: Springer.

Wearne, K.A., Winter, H.C., O'Shea, K. & Goldstein, I.J. (2006) Use of lectins for probing differentiated human embryonic stem cells for carbohydrates. *Glycobiology* **16**, 981–990.

Wobus, A.M. & Boheler, K.R. (2005) Embryonic stem cells: prospects for developmental biology and cell therapy. *Physiol. Rev.* **85**, 635–678.

Wollscheid, B., Bausch-Fluck, D., Henderson, C., O'Brien, R., Bibel, M., Schiess, R., Aebersold, R. & Watts, J.D. (2009) Mass-spectrometric identification and relative quantification of N-linked cell surface glycoproteins. *Nat. Biotechnol.* **27**, 378–386.

Wright, A.J. & Andrews, P.W. (2009) Surface marker antigens in the characterization of human embryonic stem cells. *Stem Cell Res.* **3**, 3–11.

Xu, R.H., Peck, R.M., Li, D.S., Feng, X., Ludwig, T. & Thomson, J.A. (2005) Basic FGF and suppression of BMP signaling sustain undifferentiated proliferation of human ES cells. *Nat. Methods* **2**, 185–190.

Yamada, Y., Sakurada, K., Takeda, Y., Gojo, S. & Umezawa, A. (2007) Single-cell-derived mesenchymal stem cells overexpressing Csx/Nkx2.5 and GATA4 undergo the stochastic cardiomyogenic fate and behave like transient amplifying cells. *Exp. Cell Res.* **313**, 698–706.

Yamanaka, S. (2009) A fresh look at iPS cells. *Cell* **137**, 13–17.

Yu, J., Vodyanik, M.A., Smuga-Otto, K., Antosiewicz-Bourget, J., Frane, J.L., Tian, S., Nie, J., Jonsdottir, G.A., Ruotti, V., Stewart, R., Slukvin, I.I. & Thomson, J.A. (2007) Induced pluripotent stem cell lines derived from human somatic cells. *Science* **318**, 1917–1920.

Yue, T. & Haab, B.B. (2009) Microarrays in glycoproteomics research. *Clin. Lab. Med.* **29**, 15–29.

Zanetta, J.P. & Vergoten, G. (2003) Lectin domains on cytokines. *Adv. Exp. Med. Biol.* **535**, 107–124.

Received: 3 August 2010
Accepted: 19 September 2010

Supporting Information/Supplementary material

The following Supporting Information can be found in the online version of the article:

Figure S1 List of lectins on LecChip™ and their specificity.

Figure S2 Signal intensities of each lectin on LecChip™.

Table S1 Scores of ES and EB cells by each formula

Table S2 Scores of iPS cells and their parental cells (MRC-5) by each formula

Table S3 Scores of iPS cells and their parental cells (AM936EP) by each formula

Table S4 Cell name of MRC-derived iPS cells

Table S5 Cell name of AM-derived iPS cells

Additional Supporting Information may be found in the online version of this article.

Please note: Wiley-Blackwell are not responsible for the content or functionality of any supporting materials supplied by the authors. Any queries (other than missing material) should be directed to the corresponding author for the article.

Human Molecular Genetics, 2011, Vol. 20, No. 2 **235–244**
doi:10.1093/hmg/ddq458
Advance Access published on October 14, 2010

Dystrophin conferral using human endothelium expressing HLA-E in the non-immunosuppressive murine model of Duchenne muscular dystrophy

Chang-Hao Cui[1,2], Shunichiro Miyoshi[3], Hiroko Tsuji[3], Hatsune Makino[1], Seiichi Kanzaki[1], Daisuke Kami[1], Masanori Terai[1], Harumi Suzuki[4] and Akihiro Umezawa[1,*]

[1]Department of Reproductive Biology, National Institute for Child Health and Development, Tokyo 157-8535, Japan, [2]Department of Basic Medical Science, Mudanjiang Medical College, Mudanjiang 157011, China, [3]Department of Cardiology, Keio University School of Medicine, Tokyo 160-8582, Japan and [4]Department of Pathology, Research Institute, International Medical Center of Japan, Tokyo 162-8655, Japan

Received July 13, 2010; Revised September 16, 2010; Accepted October 8, 2010

Human leukocyte antigen (HLA)-E is a non-classical major histocompatibility complex class I (Ib) molecule, which plays an important role in immunosuppression. In this study, we investigated the immunomodulating effect of HLA-E in a xenogeneic system, using human placental artery-derived endothelial (hPAE) cells expressing HLA-E in a mouse model. *In vitro* cell lysis analysis by primed lymphocytes in combination with siRNA transfection showed that HLA-E is necessary for inhibition of the immune response. Similarly, *in vivo* cell implantation analysis with siRNA-mediated down-regulation of HLA-E demonstrates that HLA-E is involved in immunosuppression. As hPAE cells efficiently transdifferentiate into myoblasts/myocytes *in vitro*, we transplanted the cells into mdx mice, a model of Duchenne muscular dystrophy. hPAE cells conferred dystrophin to myocytes of the 'immunocompetent' mdx mice with extremely high efficiency. These findings suggest that HLA-E-expressing cells with a myogenic potential represent a promising source for cell-based therapy of patients with muscular dystrophy.

INTRODUCTION

Duchenne muscular dystrophy (DMD) is a severe, recessive X-linked form of muscular dystrophy, characterized by rapid progression of muscle degeneration that eventually leads to loss in ambulation, paralysis and death. The disorder is caused by a mutation in the gene encoding dystrophin, an important structural component of muscle tissues. The absence of intact dystrophin results in destabilization of the extracellular membrane–sarcolemma–cytoskeleton architecture, making muscle fibres susceptible to contraction-associated mechanical stress and degeneration. Skeletal muscles degenerate progressively and irreversibly and are replaced by fibrotic tissues (1). Several protocols have been developed for cell-based therapies, especially using an mdx mouse model, in which mouse dystrophin is defective due to a single point mutation (2,3).

There is no known cure for DMD. However, use of stem cells or myogenic progenitors holds significant potential as an effective and suitable treatment. Myoblasts represent the natural first choice in cell-based therapy for skeletal muscle due to their intrinsic myogenic commitment. However, myoblasts recovered from muscular biopsies are poorly expandable *in vitro* and rapidly undergo senescence (1). Cells with myogenic potential are present in many other tissues, and these cells readily form skeletal muscle under favourable culture conditions (4). Indeed, cell-based therapy for damaged muscle tissue has already reached the clinical setting, with several types of cell populations being exploited (5,6). Experimental approaches to DMD using animal models have also been

*To whom correspondence should be addressed at: National Institute for Child Health and Development, 2-10-1, Okura, Setagaya, Tokyo 157-8535, Japan. Tel: +81 354947047; Fax: +81 354947048; Email: umezawa@1985.jukuin.keio.ac.jp

extensively investigated, using cells derived from bone marrow (7), synovial membrane (8) and menstrual blood (9).

In any cell-based therapy, donor cells are frequently rejected by recipients when transplanted in an allogeneic combination. Rejection is caused by a mismatch of the human leukocyte antigen (HLA). There are a large number of different alleles of each HLA, so a perfect match of all HLAs between donor cells and host cells is extremely rare. HLA-E, together with HLA-G and HLA-F, is a non-classical major histocompatibility complex class I (MHC Ib) molecule (10), which plays an important role in immunosuppression. Among Ib molecules, HLA-E exhibits a restricted pattern of expression in different cell types (11) and is a ligand of CD94/NKG2 receptors (12,13). The interaction of HLA-E with the inhibitory CD94/NKG2 receptor results in the inhibition of natural killer (NK) cell- and cytotoxic T lymphocyte-dependent lysis (12,14). Uteroplacental immune privilege systems utilize this immunosuppression through production of HLA-E, HLA-F and HLA-G in the uterus and the placenta.

In this study, we investigated the immunomodulating effect of HLA (class Ib) in a xenogeneic combination, using placenta-derived cells expressing HLA-E. Human placental artery-derived endothelial (hPAE) cells conferred dystrophin to myocytes of 'immunocompetent' mdx mice, a model of DMD, doing so with extremely high efficiency.

RESULTS

Derivation of hPAE cells

We successfully cultured a large number of hPAE cells obtained from placental arteries of five donors by the explant culture method (Fig. 1A; see Materials and Methods). hPAE cells with endothelium-like morphology (Fig. 1B) adhered to dishes and were regarded as being population doubling (PD) 0 at day 2. They continued to proliferate until PD 17 at day 20 (Fig. 1C). Cell proliferative capacity was assessed by calculating the total number of PDs (PD level or accumulative PDs) using the formula $\log_{10}$(total number of cells/starting number of cells)/$\log_{10}$ 2. Flow cytometric analysis revealed that hPAE cells were positive for CD29 (integrin b1), CD31 (PECAM-1), CD44 (Pgp-1/ly24), CD59, CD73, CD105 and CD166 (ALCAM) and negative for CD45, CD106 (VCAM-1) and CD117 (c-kit) (Fig. 1D and E). Almost all the cells were positive for the endothelial marker CD31 (97.7%), implying that the cells were of endothelial origin. Reverse transcriptase (RT)–polymerase chain reaction (PCR) analysis revealed that hPAE cells expressed the endothelial markers constitutively (Fig. 1F). Immunocytochemical analysis also indicated that the hPAE cells were positive for CD31 and von Willebrand factor (vWF) (Fig. 1G). We next tested whether hPAE cells would form an 'angiogenesis network' when plated on Matrigel. As shown in Figure 1H, culture of hPAE cells on extracellular matrix resulted in vascular tube formation within 6 h. hPAE cells with vascular tube formation were immunocytochemically positive for vascular endothelial growth factor (VEGF) (Supplementary Material, Fig. S1).

Expression of HLA-E in hPAE cells

Since non-classical MHC is involved in immune privilege (10,15), we investigated whether hPAE cells produce HLA-E after exposure to cytokines (16). hPAE cells started to express HLA-E after exposure to cytokines at the transcriptional level (Fig. 2A) and the protein level (Fig. 2B and C). Immunostaining showed that HLA-E was mainly localized in the cytoplasm (Fig. 2B, right). Western blot analysis using anti-HLA-E-specific monoclonal antibody revealed a single discrete band at 42 kDa, consistent with the molecular weight of HLA-E protein (Fig. 2C). Immunoprecipitation analysis of the cell supernatant showed a single band at 37 kDa, consistent with the molecular weight of soluble HLA-E (sHLA-E) protein (Fig. 2D), implying that sHLA-E is secreted.

Myogenic induction of hPAE cells *in vitro*

We then investigated whether hPAE cells are capable of differentiating into skeletal myocytes *in vitro* (Fig. 3). hPAE cells started to exhibit multinucleated myotubes in culture after induction (Fig. 3A). Immunocytochemistry indicated that enhanced green fluorescent protein (EGFP)-labelled multinucleated myotubes were positive for desmin (Fig. 3B) and myosin heavy chain (Fig. 3C and D). Myogenesis of hPAE cells was also analysed by RT–PCR with primers that can amplify human myogenic genes, but not their mouse counterparts. hPAE cells constitutively expressed the myogenin gene and started to express the desmin and MyHC-IIx/d genes after induction (Fig. 3E). We also performed tartrate-resistant acid phosphatase stain for osteoclasts, alkaline phosphatase stain for osteoblasts and Oil red O stain for adipocytes on hPAE cells at 21 days after the start of co-cultivation (Supplementary Material, Fig. S2), but failed to detect positive reaction by these stains.

Direct implantation of hPAE cells into immunocompetent BALB/c mice

To further evaluate the *in vivo* response to hPAE cells, cells were directly injected into the thigh muscles of immunocompetent BALB/c mice (17). For comparison, periosteal cells with low expression of HLA-E were injected in the same manner. Histopathological analysis revealed that the injection of periosteal cells induced an immune response at the injected site (Fig. 4A), but hPAE cells did not (Fig. 4B), suggesting that hPAE cells fail to elicit pro-inflammatory responses in immunocompetent mice. Immunohistochemical analysis, using an antibody specific to human vimentin, revealed that the hPAE cells extensively migrated between muscular fibres (Fig. 4B, lower panels). Immunofluorescent analysis revealed that CD45 and CD3 lymphocytes infiltrated near the (donor) periosteal cells at 2 days after the injection into the Balb/c muscle, and the number of lymphocytes increased at 2 weeks (Fig. 4C). In contrast, CD45- and CD3-positive cells were not detected around the vimentin-positive hPAE cells at 2 weeks. We also performed immunofluorescent analysis and western blot analysis to investigate the expression of HLA-E *in vivo*. hPAE cells expressed HLA-E in the muscle tissues (Fig. 4D and E). Moreover, HLA-E expression

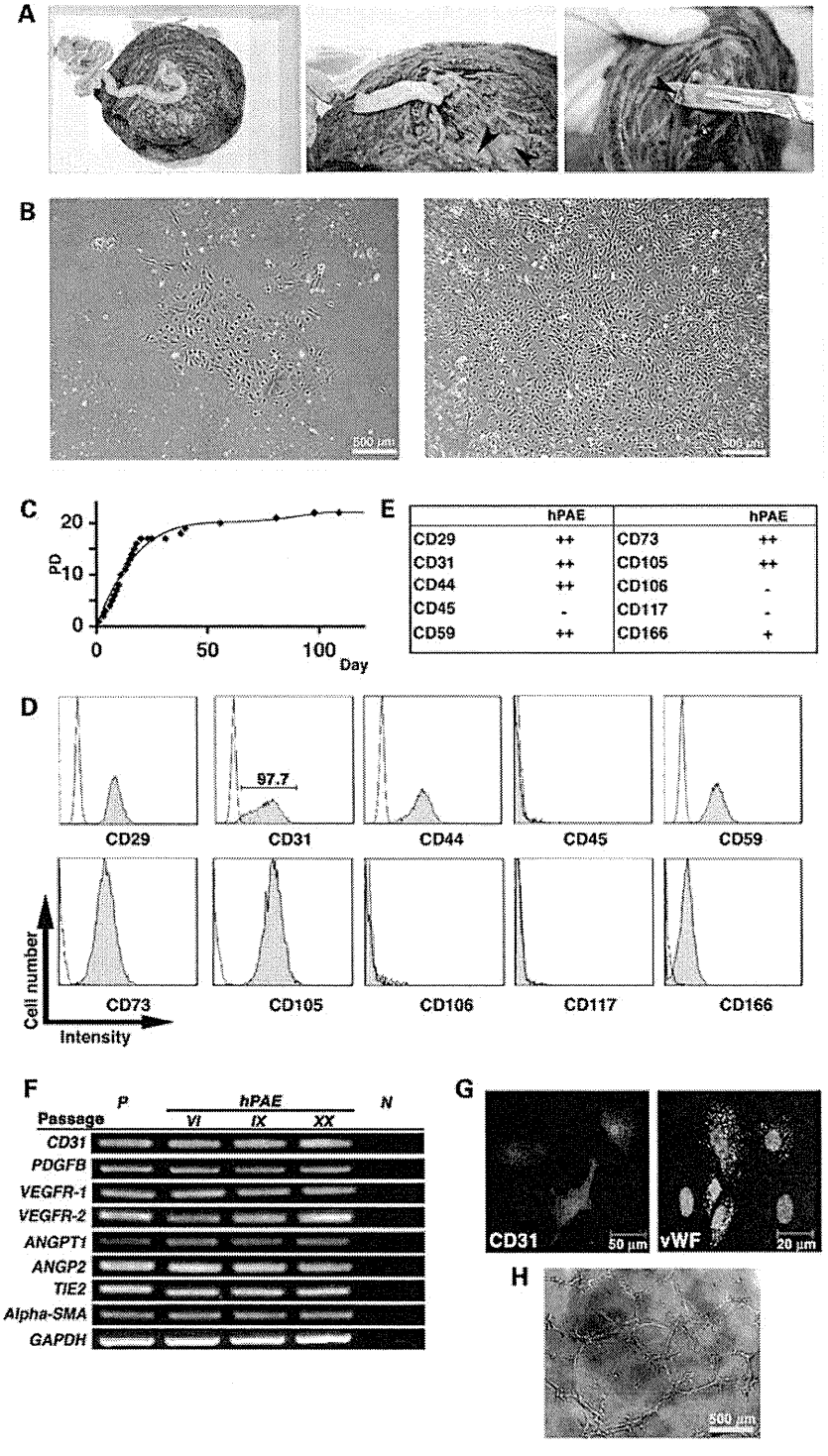

Figure 1. *In vitro* characterization of hPAE cells. (**A**) Macroscopic views showing an explant culture method of hPAE cells. hPAE cells were dissected from isolated placenta arterial vessels (indicated by arrowheads) in human placenta. (**B**) Photos showing morphology of hPAE cells by phase contrast microscopy at primary stages at passage I (left panel: PD 0 and right panel: PD 3). (**C**) Proliferative capacity of hPAE cells. The number of cells was counted with ViCell (Beckman Coulter) at each passage. The total number of PDs (PD level or accumulative PDs) was calculated, using the formula $\log_{10}$(total number of cells/starting number of cells)/$\log_{10}$ 2. (**D**) Flow cytometric profiles indicating expression of several cell surface markers on hPAE cells. (**E**) Scores of peak intensity, compared with isotype controls. '++': strongly positive (10 times and above that of the isotype control), '+': weakly positive (<10 times and twice and above that of the isotype control), '−': negative (less than twice that of the isotype control). (**F**) RT–PCR analysis for endothelial marker expression in hPAE cells at passage VI, IX and XX. The cells were cultured without any inductive stimuli. RNAs from HUVECs and H_2O serve as positive (P) and negative (N) controls, respectively. (**G**) Immunocytochemical analyses of CD31 and vWF in hPAE cells. (**H**) Phase contrast micrograph of *in vitro* endothelial network formation of hPAE cells. hPAE cells were cultured on a basement membrane matrix gel. An 'angiogenesis network' was formed 6 h after cultivation began.

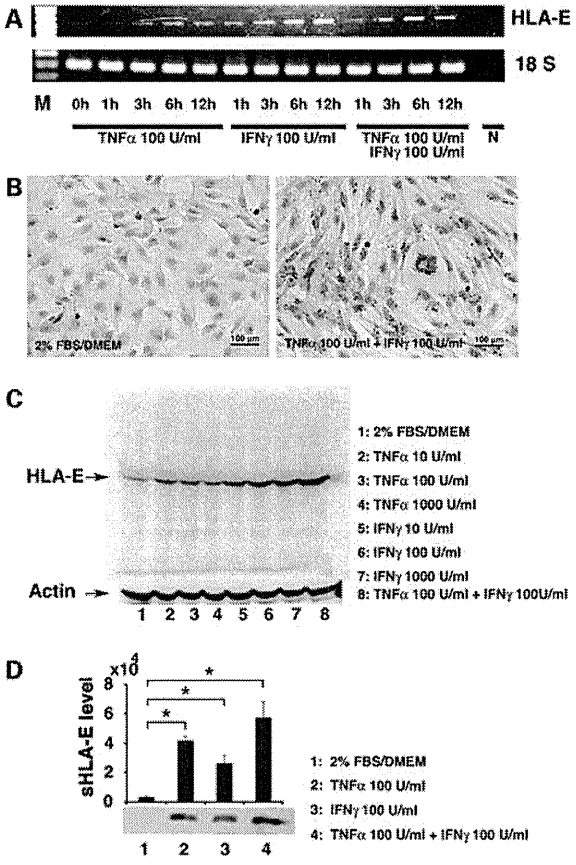

Figure 2. HLA-E mRNA and protein in hPAE cells upon treatment with tumor necrosis factor α (TNFα) and interferon γ (IFNγ). (**A**) RT–PCR showing a time-course of HLA-E expression in response to TNFα and IFNγ. 18S RNA was used as a loading control. M = size markers and N = a negative control in PCR with H_2O. (**B**) Immunocytochemistry of HLA-E localization. The cells were incubated for 24 h with a combination of TNFα and IFNγ at the indicated concentrations (right). Left panel = untreated control. (**C**) Western blot analysis of cell lysates showing levels of HLA-E at 24 h after treatment with TNFα and IFNγ. Combination of two reagents induced more HLA-E at the protein level. Actin was used as a loading control. (**D**) Immunoprecipitation analysis of culture supernatants showing a soluble form of HLA-E (sHLA-E) with exposure to TNFα and IFNγ. sHLA-E level was determined by each signal intensity (mean ± SE). $n = 3$, $^*P < 0.05$.

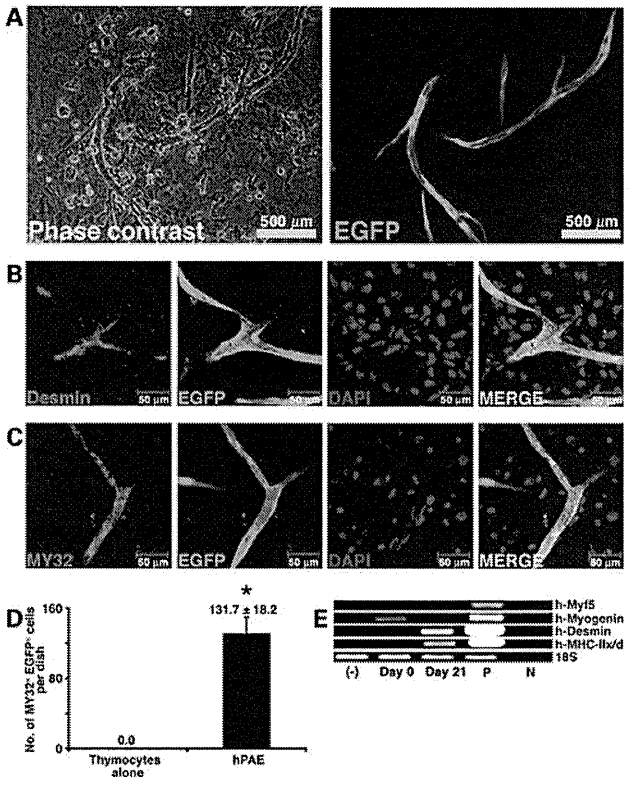

Figure 3. Myogenic differentiation of hPAE cells under cell culture conditions. (**A**) Photos showing myogenic differentiation of hPAE cells detected by phase contrast microscopy (left) and by fluorescent microscopy (right) in an identical area. EGFP-labelled hPAE cells co-cultured with neonatal murine thymocytes for 21 days. (**B** and **C**) Immunocytochemistry of hPAE cells expressing myogenic markers, desmin (B) and skeletal myosin heavy chain (C, MY32). (**D**) Quantitative analysis of MY32-positive hPAE cells. MY32- and EGFP-double positive cells (no. of MY32+ EGFP+ cells) were counted in 35 mm dishes 3 weeks after induction (mean ± SE). $n = 3$, $^*P < 0.05$. (**E**) RT–PCR showing myocyte-specific genes were expressed along with myogenic differentiation. RT–PCR analysis with PCR primers that amplify only human mRNAs of Myf5, myogenin, desmin and MyHC-IIx/d, but not murine mRNAs. RNAs from human muscle and H_2O served as positive (P) and negative (N) controls, respectively.

remained unchanged over 6 weeks. We then examined interleukin-4 (IL-4), which is essential for transplantation immunity. IL-4 production reached a maximum level after 2 weeks at the injected site and then decreased (Supplementary Material, Fig. S3).

To investigate whether hPAE cells can generate muscle tissue *in vivo*, hPAE cells were implanted directly into the right thigh muscles of BALB/c mice, with phosphate-buffered saline (PBS) being injected at the contralateral muscles as a control. Immunohistochemical analysis was performed using the human-specific antibody at 3 weeks after injection. Myotubes at the injected site expressed human dystrophin as a cluster. No positive reaction was detected in the muscle of BALB/c mice without cell implantation (PBS alone) (Fig. 4E and F; Supplementary Material, Fig. S4). These results imply that dystrophin is transcribed from the dystrophin gene of human donor cells after hPAE cells differentiated into myotubes and fused to host myocytes without immune response. To determine whether human dystrophin expression in the donor cells is caused by fusion, immunohistochemistry with an antibody against human nuclei (Ab-HuNucl) and 4′,6-diamidino-2-phenylindole (DAPI) stain was performed. We examined almost all the 7 mm thick serial histological sections parallel to the muscular bundle (cross-section) of the muscular tissues by confocal microscopy and found that myocytes had nuclei derived from both human and murine cells in the cross-section (Fig. 4G), implying that dystrophin expression is attributed to fusion between murine host myocytes and human donor cells.

Inhibition of HLA-E by small interfering RNA (siRNA)

To investigate the involvement of HLA-E in immunosuppression, we suppressed HLA-E expression by siRNA in hPAE cells. A significant decrease in HLA-E mRNA was observed

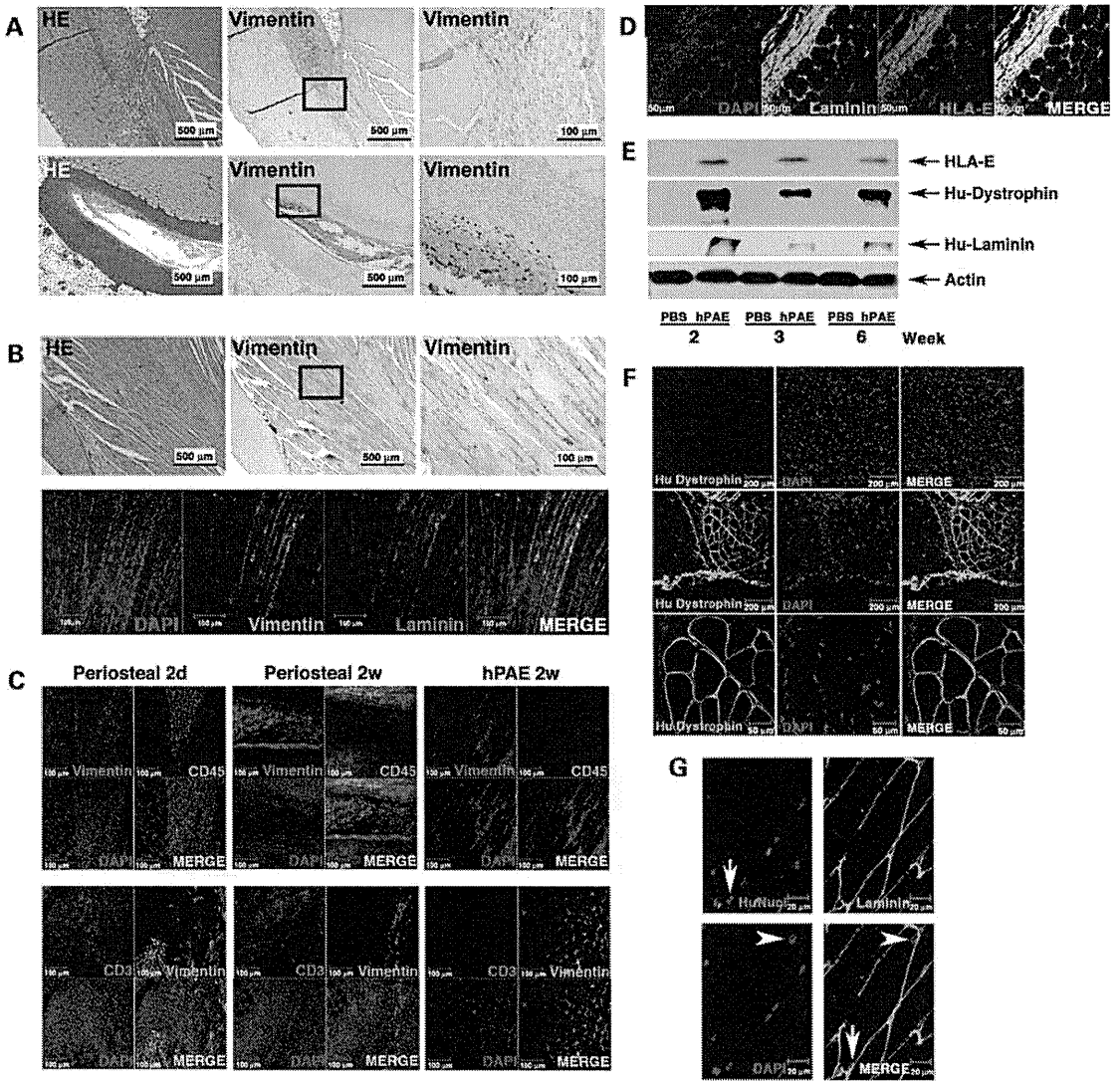

Figure 4. Implantation of hPAE cells into the thigh muscle of BALB/c mice. (**A**) Human periosteal cells (2×10^7 cells) were injected directly into the thigh muscles of BALB/c mice. Immunohistochemical analysis was performed on the muscle section using an antibody against vimentin. Upper panels: 2 days after injection and lower panels: 2 weeks after injection. (**B**) hPAE cells (2×10^7 cells) were injected directly into the thigh muscles of BALB/c mice. Upper panels: immunohistochemistry against vimentin. Lower panels: immunofluorescent analysis. DAPI (blue), vimentin (green), laminin (red) and MERGE (from left to right). (**C**) Immunohistochemical analysis of the thigh muscle sections at 2 days or 2 weeks after injection of human periosteal cells (hPeriosteal) and at 2 weeks after injection of hPAE cells, using antibodies against vimentin (upper panels: red and lower panels: green), leukocyte marker CD45 (green) and T cell marker CD3 (red). (**D**) Immunofluorescent analysis using an antibody against HLA-E (red) and human laminin (green) on the thigh muscle sections at 2 weeks after injection of hPAE cells. (**E**) Western blot analysis of muscle lysates showing levels of HLA-E, dystrophin and laminin. BALB/c mice were implanted with PBS or hPAE cells at the indicated weeks. The level of actin protein was used as a loading control. (**F**) Immunofluorescent analysis using an antibody against human dystrophin (green) on thigh muscle sections 3 weeks after direct injection of hPAE cells (middle and lower panels). PBS was injected into contralateral muscles as a control (upper panels). Dystrophin is totally absent in PBS-injected muscles (upper panels), whereas clusters of muscle fibres display peripheral localization of the dystrophin protein in mice injected with hPAE cells (middle and lower panels). Dystrophin (green), DAPI (blue) and MERGE (from left to right). (**G**) Immunofluorescent analysis using antibodies against laminin (green), human nuclei (HuNucl, red, arrows) and DAPI staining (blue, arrowheads) on thigh muscle sections 3 weeks after injection of hPAE cells.

in the cells transfected with HLA-E siRNA (siHLA-E) when compared with control cells (Fig. 5A). In the same set of experiments, HLA-E protein decreased significantly in siHLA-E-transfected cells when compared with control cells (Fig. 5B). To investigate the involvement of HLA-E in *in vivo* immune response, after pre-treatment with 20 μM siHLA-E for 48 h, hPAE cells were injected into the thigh muscles of immunocompetent BALB/c mice, with hPAE cells treated with control siRNA being injected into the contralateral muscles as a control (Fig. 5C–F). Histopathological analysis revealed that injection of siHLA-E-treated hPAE cells elicited an immune response, as revealed by infiltration of CD3- and CD45-positive lymphocytes in immunocompetent BALB/c mice 7 days after injection, whereas injection of

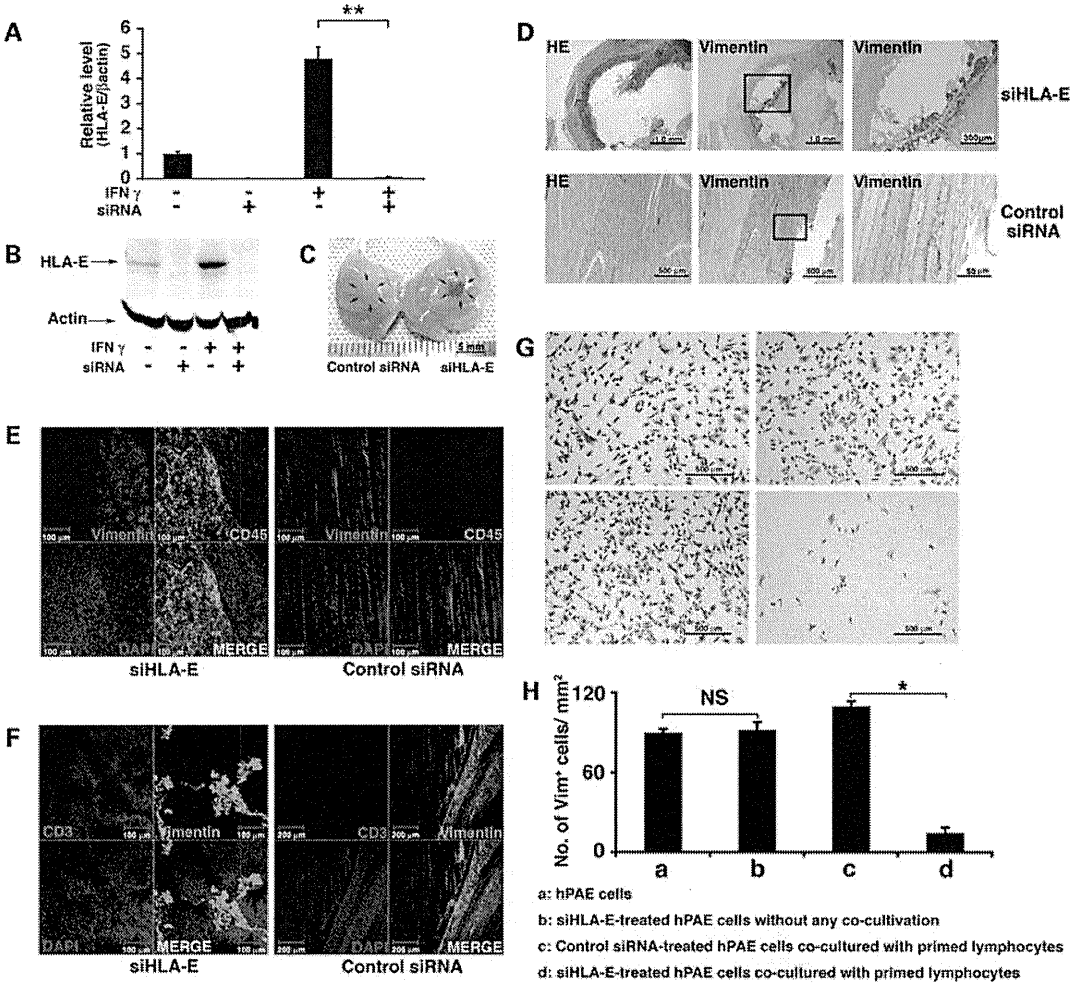

Figure 5. Functional effect of HLA-E siRNA on immunosuppression. (**A**) Inhibition of HLA-E mRNA by siRNA. hPAE cells (1×10^4) grown on 6-well plates were transfected with either control siRNA or HLA-E-specific siRNA (20 μM) for 48 h. HLA-E mRNA levels were quantified using RT–PCR, normalized to β-actin (mean ± SE). $n = 3$, $^{**}P < 0.01$. (**B**) Inhibition of HLA-E protein by siRNA. Whole-cell protein extracts were analysed by SDS–PAGE immunoblotting with antibodies to HLA-E and actin. (**C**–**F**) siHLA-E-treated hPAE cells and control siRNA-treated hPAE cells were injected into the right and left thigh muscle of BALB/c mice, respectively. Mice were sacrificed 7 days after injection. (C) Injected sites are indicated by arrows (left: control siRNA and right: HLA-E-specific siRNA). (D) Microscopic view (HE stain and immunohistochemistry) of thigh muscles implanted with siHLA-E-treated (upper panels) or control siRNA-treated (lower panels) hPAE cells. (E and F) Immunohistochemical analysis of thigh muscle sections, after injection of siHLA-E-treated or control siRNA-treated hPAE cells and staining with antibodies against vimentin (E: red and F: green), leukocyte marker CD45 (E: green) and T cell marker CD3 (F: red). (**G**) Induction of xenoreactive lysis with spleen-derived lymphocytes. siHLA-E-treated hPAE cells or control siRNA-treated hPAE cells were co-cultured with spleen-derived lymphocytes and immunocytochemically stained for human vimentin. (G) Upper left: hPAE cells, upper right: siHLA-E-treated hPAE cells without any co-cultivation, lower left: control siRNA-treated hPAE cells co-cultured with primed lymphocytes, lower right: siHLA-E-treated hPAE cells co-cultured with primed lymphocytes. (**H**) Survival of hPAE cells after xenoreactive analysis. Vimentin-positive cells (no. of vimentin+ cells/mm^2) significantly decreased in siHLA-E-treated cells when compared with control siRNA-treated cells 3 days after co-incubation with primed lymphocytes. $^{*}P < 0.01$, NS = not significant.

control siRNA-treated hPAE cells did not (Fig. 5E and F). This suggests that HLA-E is necessary for inhibition of an immune reaction *in vivo*. We then investigated whether lysis of hPAE cells by primed lymphocytes is mediated by HLA-E. hPAE cells treated with either siHLA-E or control siRNA were co-cultured with spleen-derived lymphocytes, and induction of xenoreactive lysis was quantified (Fig. 5G and H). siHLA-E-treated hPAE cells were lysed by primed lymphocytes, whereas control siRNA-treated hPAE cells were not, indicating that HLA-E is also necessary for inhibition of the immune response *in vitro*.

Conferral of human dystrophin by cell implantation in the mdx mouse

To investigate whether hPAE cells can confer human dystrophin to myocytes, untreated EGFP-labelled cells were implanted directly into the thigh muscles of mdx mice (Fig. 6A). PBS was injected into the contralateral muscles as a control (Fig. 6B). At 3 weeks after implantation, human dystrophin was detected in EGFP-positive myotubes as a cluster at 18.2% (Fig. 6C). Expression of dystrophin was not caused by reversion to the normal phenotype of dystrophied myocytes

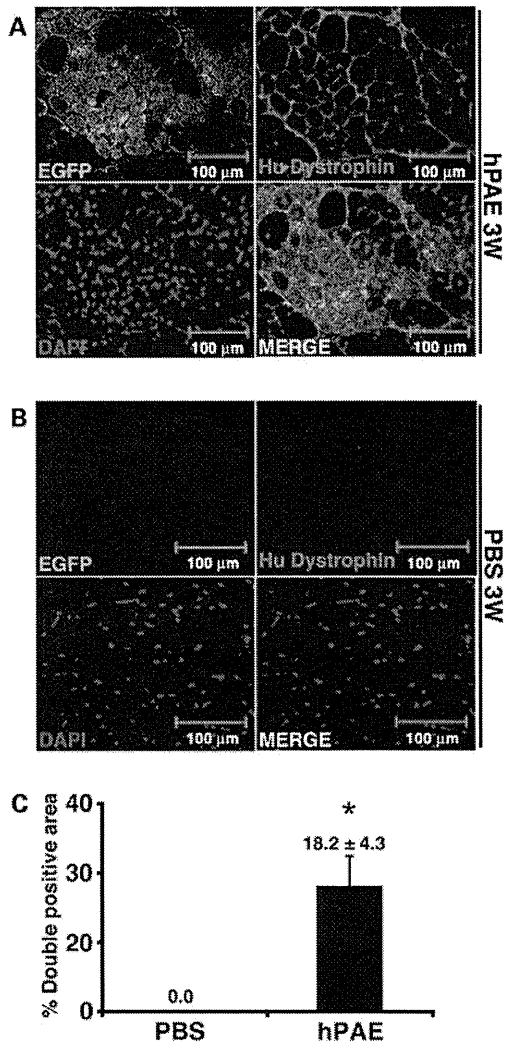

Figure 6. Conferral of dystrophin to mdx myocytes by hPAE cells. (**A**) EGFP-labelled hPAE cells were injected into the thigh muscle of mdx mice. Immunohistochemical analysis revealed the incorporation of implanted cells into newly formed EGFP-positive myofibres (green), which expressed human dystrophin (red) 3 weeks after implantation. (**B**) PBS was injected into contralateral muscles as a control. (**C**) Quantitative analysis of human dystrophin-positive myotubes. The percentage of human EGFP- and dystrophin-positive myofibre areas (% double positive area) was calculated 3 weeks after injection of cells or PBS (mean ± SE). $n = 3$, $^*P = 0.05$.

in the mdx mice because the antibody used in this study is specific to humans. These results suggest that human dystrophin is transcribed from the dystrophin gene of human donor cells.

DISCUSSION

DMD is a devastating X-chromosome-linked muscle disease characterized by progressive muscle weakness attributable to a lack of dystrophin expression at the sarcolemma of muscle fibres (18). There are currently no effective therapeutic approaches for muscular dystrophy. hPAE cells have a high replicative ability, similar to progenitors or stem cells that display a long-term self-renewal capacity, and had a much higher growth rate in our experimental conditions than marrow-derived stromal cells (19). Immunosuppressive hPAE cells with a direct myogenic potential thus offer significant potential for novel, effective and sustainable cell-based therapy, including when being used in an allogeneic manner. The function of HLA-E has been fully elucidated through its interaction with CD94-NKG2 receptors expressed on NK cells and a subset of T cells (12,13). *In vitro* studies using human cells provided evidence of HLA-E involvement in negative signalling to immune responses (20). Qa-1 (homologous to HLA-E in mice)-deficient mice have defects in immunoregulation mediated by T cells (21). Survival of donor cells in an immunocompetent mouse is attributed, at least partially, to HLA-E-dependent immunosuppression, because knockdown experiments of HLA-E clearly indicate involvement of HLA-E in cell-mediated lysis of hPAE cells (Fig. 5). HLA-E is a protective response of hPAE cells to injury and plays an important role in immunosuppression, irrespective of being either the membrane-bound or soluble form.

It is noteworthy that hPAE cells, as well as other placenta-derived cells, are obtained by a simple, safe and painless procedure, and a large number of hPAE cells can easily be harvested from placental arteries. In this study, we manually separated chorionic large arteries from the chorionic plate that entirely covers the foetal surface of the placenta, which is, in turn, covered by the aminion (Fig. 1A). hPAE cells proliferate over at least PD 17 for >20 days and stop dividing before PD 22. The predicted number of CD31-positive hPAE cells from one placenta of an average size (500 g) would be 1×10^7 (before *ex vivo* amplification), possibly reaching 1×10^{12} after cultivation. This may cover 30 000 cm^3 of muscular tissues in cell-based therapy (5). Cells converted into myotubes *in vitro* at a high frequency after induction, giving rise to large numbers of myofibres expressing human dystrophin when transplanted into BALB/c and mdx mice, thus fulfilling all the criteria required for a successful allogeneic cell therapy for muscular dystrophy.

Compared with previously reported experiments, including from our laboratory (9), the frequency of myotubes with human dystrophin after cell implantation was extremely high. In addition to *in vivo* myogenesis, *in vitro* myogenesis was induced. Myogenin, a helix–loop–helix transcription factor, determines muscle cell fate and accelerates cell fusion, and is constitutively expressed in hPAE cells, implying either that these cells have myogenic potential or that these cells are myogenic progenitors, although their origin is endothelial from the viewpoint of isolation procedure and cell surface markers. Myogenesis may also be promoted by cytokines such as VEGF (22) as well as transcription factors. Furthermore, in cases of cell-based therapy, the so-called 'space' is necessary for survival of implanted donor cells. Irradiation has been used for the generation of space in cases of bone marrow transplantation. Toxin, to induce muscle injury and pathophysiological ischaemia of muscular tissues, can also generate space in muscle (23). BALB/c and mdx mice were used in this study, and almost identical results were obtained from both mice types, although BALB/c mice theoretically do not have any muscular injury. High frequency of human

dystrophin-positive myotube formation may be attributed to the generation of space by the immune response after cell implantation in a xenogeneic combination. hPAE cells produce HLA-E after immunoreaction by production of immunocytokines such as IL-4 (Supplementary Material, Fig. S1), followed by induction of immunosuppression through HLA-E. This immune reaction after cell implantation possibly generates space to enable survival of implanted cells. This possibility is rather favourable because any future cell-based therapy for DMD patients will be employed in an allogeneic combination. In contrast, experimental approaches have been tested in a syngeneic combination, in immunodeficient mice or via use of immunosuppressive drugs. Clinical trials in humans, use an allogeneic combination (5,6), are in no way inferior compared with experimentation with the murine model systems. This study may explain the high frequency of donor cell survival at the implanted sites observed in clinical trials.

Induction of immunosuppression via HLA-E from hPAE cells observed in this study directly leads to the possibility of clinical, allogeneic cell-based therapy. Mesenchymal stem cells (MSCs) or mesenchymal progenitors, isolated from bone marrow as an adherent fibroblast-like population (24), have already been identified in many tissues, including umbilical-cord blood (25), the placenta (26), fat and amniotic fluid (27). They have been used for cell-based therapy because of their self-renewal capacity and their ability to form bone, fat, cartilage, muscle, cardiocytes and neurons (28,29). The isolation of tissue-specific stem cells for expansion *in vitro* and transplantation back into the patient in an allogeneic manner is an ideal strategy, from the viewpoint of industry-based, sustainable supply of large quantities of affordable, quality-controlled cells. Using autologous MSCs to restructure damaged tissues has had some clinical success (30). In most cases of degenerative and genetic diseases, it is unlikely that enough unaffected stem cells will be isolated or available in sufficient quantity, necessitating the use of stem cells from suitable, cost-effective allogeneic sources such as placenta.

MATERIALS AND METHODS

Cultivation of hPAE cells

Human placentas were collected, after delivery, with informed consent. Ethical approval was granted by the Institutional Review Board. To isolate arterial endothelium, we used the explant culture method, in which the cells were outgrown from pieces of placenta arterial vessels (Fig. 1A). Briefly, arterial vessels were separated from arteries in the chorionic plate and chopped into $\sim 5\ mm^3$ pieces. The pieces were washed in endothelial basal medium (EBM)-2 (Cambrex, Walkersville, MD, USA) and cultured in endothelial growth medium-2 MV (EGM-2MV; Cambrex), which consisted of EBM-2, 5% foetal bovine serum (FBS) and supplemental growth factors including VEGF, basic fibroblast growth factor, epidermal growth factor and insulin-like growth factor. Arterial vessels attached to the substratum of culture dishes (BD Falcon; Becton Dickinson and Company, San Jose, CA, USA), and cells migrate out from the surface of tissues after 20 days of incubation at 37°C in 5% CO_2. The cells were harvested with PBS, with 0.1% trypsin and 0.25 mM EDTA, and were re-seeded at a density of 3×10^5 cells in a 10 cm diameter dish. Confluent monolayers of cells were further subcultured. The culture medium was replaced every 3–4 days.

In vitro lentivirus-mediated gene (EGFP) transfer into hPAE cells

Infection of cultured hPAE cells with lentivirus (having a CMV promoter-regulated EGFP reporter plasmid) resulted in high levels of EGFP expression in all cells. EGFP expression was analysed by flow cytometry (31).

Flow cytometric analysis

Flow cytometric analysis was performed as described previously (9). Cells were incubated with primary antibodies or isotype-matched control antibodies followed by immunofluorescent secondary antibody staining. Cells were analysed on an EPICS ALTRA analyser (Beckman Coulter, Fullerton, CA, USA). Antibodies against human CD29, CD31, CD44, CD45, CD59, CD73, CD105, CD106, CD117, CD166 and VEGER (Flk-1) were purchased from Beckman Coulter, Immunotech (Marseille, France), Cytotech (Hellebaek, Denmark) and BD Biosciences Pharmingen (San Diego, CA, USA).

Myogenic differentiation of hPAE cells

A cell suspension was prepared from neonatal murine thymi using frosted slide glasses (MUTO-Glass, Japan). The thymocyte suspension was then washed once in PBS with 2% FBS and filtered through a 100 μm nylon mesh. After centrifugation at 1000 rpm for 5 min, the cell pellet was re-suspended in 10% FBS/Dulbecco's modified Eagle's medium. Floating thymocytes were collected and re-plated at $1 \times 10^6/cm^2$. The next day, hPAE cells were harvested with 0.25% trypsin and 1 mM EDTA and overlaid onto the cultured neonatal thymocytes at $1 \times 10^4/cm^2$. The culture medium was replaced every 2 days with fresh EGM-2 MV.

RT–PCR analysis

Total RNAs (2 μg) were reverse-transcribed with oligo (dT), as described previously (9), and RT–PCR was carried out with primer sets specific for human Myf5, myogenin, desmin, myosin heavy chain-IIx/d (MyHC-IIx/d) (primer sequences are shown in Supplementary Material, Table S1). Human muscle RNAs and H_2O served as positive (P) and negative (N) controls, respectively. The 18S PCR primers were used as a positive control for both human and murine cDNAs. The HLA-E primers (F: CCACCATGGTAGATG GAACCC and R: GCTTTACAAGCTGTCAGACTC) used were the same as those described previously (16). The primer sequences of endothelial cell markers are listed in Supplementary Material, Table S1. Human umbilical vein endothelial cell (HUVEC) RNAs and H_2O served as positive (P) and negative (N) controls, respectively. Glyceraldehyde phosphate dehydrogenase was also used as a positive control.

For quantitative analysis of mRNA levels for HLA-E, the total RNAs were isolated from HLA-E-specific siRNA or control siRNA-transfected hPAE cells using an RNeasy mini-kit (Qiagen, Chatsworth, CA, USA) and were reverse-transcribed by TaKaRa recombinant Taq (Takara Bio Inc., Japan). Real-time PCR was carried out with an ABI PRISM 7000 Sequence Detection System. The 25 μl reaction mixture contained 12.5 μl of SYBR Green PCR Master Mix (TOYOBO, Japan), 10 ng of cDNA template and a primer set for HLA-E, F: CGGCTACTACAATCAGAGCGA and R: CACGCATGTGTCTTCCAGG or for β-action, F: CATGTACGTTGCTATCCAGGC and R: CTCCTTAATGTCACGCACGAT. The relative quantification of the transcripts was analysed using the comparative threshold cycle method supplied by the manufacturer.

Immunohistochemical and immunocytochemical analyses

For immunohistochemical analysis (19), the skeletal muscle tissue section slides (paraffin-embedded) were incubated with anti-vimentin monoclonal antibody (clone: V9, Dakocytomation, Glostrup, Denmark) for 1 h at room temperature, followed by horseradish peroxidase (HRP)-conjugated secondary antibody. Staining was detected by diaminobenzidine and H_2O_2. Slides were counterstained with haematoxylin. For the immunofluorescence, antibodies against human dystrophin (NCL-DYS3, Novocastra, Newcastle upon Tyne, UK), GFP (Catalogue no. 632377, Clontech, Mountain View, CA, USA), human nuclei (Catalogue no. MAB1281, Chemicon, Temecula, CA, USA), HLA-E (clone 4D12, MBL, Japan), vimentin, CD45 (leukocyte common antigen) (clone 30-F11, Invitrogen, Camarillo, CA, USA), CD3 (Catalogue no. sc-1127, Santa Cruz Biotechnology, Santa Cruz, CA, USA) and laminin (Mob 202, clone 4C7, DBS, CA, USA; 4H8-2, ab11576, Abcam plc, Cambridge, UK) were used as first antibodies, followed by Alexa-Fluor-conjugated secondary antibodies (Molecular Probes, Eugene, OR, USA).

Immunocytochemical analysis was performed as described previously (19). The antibodies against CD31 (Catalogue no. SCR023, Part no. 2003788, Chemicon), vWF (Catalogue no. SCR023, Part no. 2003787, Chemicon), VEGF (clone EP1176Y, Abcam plc), desmin (clone D9, Catalogue no. 010031, BioScience Products, Emmenbruecke, Switzerland), skeletal myosin (clone MY-32, Sigma-Aldrich, Inc., St Louis, MO, USA), GFP and vimentin were used as first antibodies and Alexa-Fluor-conjugated goat anti-mouse (rabbit) IgG and HRP-conjugated rabbit anti-mouse IgG were used as second antibodies.

Western blotting and immunoprecipitation

Western blot analysis was performed as described previously (19). Blots were incubated with primary antibodies for HLA-E (clone MEM-E/02, Serotec, Oxford, UK), laminin (Mob 202, clone 4C7, DBS) or dystrophin (NCL-DYS3, Novocastra) for 1–2 h at room temperature. After washing, blots were incubated with an HRP-conjugated secondary antibody (0.04 μg/ml) for 30 min. The blots were developed with enhanced chemiluminescence substrate, according to the manufacturer's protocol.

For immunoprecipitation, the supernatants of hPAE cell were incubated with HLA-E antibody (1–2 μg for each sample) for 1 h, followed by incubation with 20 μl of protein A/G plus agarose overnight at 4°C. The supernatants were removed by centrifugation, and the pellets were boiled in 2× sample buffer for 4 min. The products were then applied to sodium dodecyl sulphate (SDS)–polyacrylamide gel electrophoresis (PAGE).

siRNA study

The HLA-E siRNA pool (HLA-E-HSS104836, HLA-E-HSS104837 and HLA-E-HSS104838) was purchased from Invitrogen (Carlsbad, CA, USA) and transfected into hPAE cells using Lipofectamine™ RNAiMAX (Invitrogen). Cells were harvested 48 h after transfection and analysed by real-time PCR and western blot.

Xenoreactive immune response

Lymphocytes from BALB/c mouse spleen were isolated by Ficoll/Histopaque density gradient centrifugation. hPAE cells were transfected with either control siRNA or HLA-E-specific siRNA (20 μM) for 48 h. The two cell populations were then co-cultured for 3 days in 2 ml of RPMI supplemented with 10% FBS and 10 U/ml IL-2 (Catalogue no. 212-12, Peprotech Inc., Rocky Hill, NJ, USA). Induction of xenoreactive lysis in the spleen-derived lymphocytes was quantified by immunostaining with a human-vimentin-specific antibody.

In vivo cell implantation

hPAE cells were implanted into the thigh muscle of 4- to 6-week-old BALB/c (Sankyo Labo Service Corporation, Hamamatsu, Japan) or mdx (C57BL/10ScSn-Dmdmdx/J, Jax Labs, Bar Harbor, ME, USA) mice. For comparison, human periosteal cells were used. The cells (2×10^7) were suspended in PBS in a total volume of 100 μl and injected directly into the thigh muscles. The mice were examined 2 days or 1, 2, 3, 4 and 6 weeks after injection by immunohistochemistry with antibodies against HLA-E, vimentin, laminin and dystrophin. The antibodies for vimentin and dystrophin (NCL-DYS3) are human tissue specific; therefore, they do not react with murine tissues or murine tissue-derived proteins. In addition, siHLA-E (20 μM)-treated or control siRNA-treated hPAE cells were injected directly into the thigh muscle of BALB/c mice.

Statistical analysis

Statistical analysis was performed using the Student's *t*-test. A 95% confidence limit was taken as significant.

SUPPLEMENTARY MATERIAL

Supplementary Material is available at *HMG* online.

ACKNOWLEDGEMENTS

We would like to express our sincere thanks to M. Yamada for fruitful discussion and critical reading of the manuscript, H. Abe for providing expert technical assistance and to K. Saito for secretarial work.

Conflict of Interest statement. None declared.

FUNDING

This work was supported by Grants-in-Aid from the Japan Society for the Promotion of Science (21659092 and 22616011) and the Intramural Research Grant (19B-7 and 22-5) for Neurological and Psychiatric Disorders of NCNP. Funding to pay the Open Access publication charges for this article was provided by the Intramural Research Grant (22-5) for Neurological and Psychiatric Disorders of NCNP.

REFERENCES

1. Cossu, G. and Mavilio, F. (2000) Myogenic stem cells for the therapy of primary myopathies: wishful thinking or therapeutic perspective? *J. Clin. Invest.*, **105**, 1669–1674.
2. Hoffman, E.P., Brown, R.H. Jr and Kunkel, L.M. (1987) Dystrophin: the protein product of the Duchenne muscular dystrophy locus. *Cell*, **51**, 919–928.
3. Sicinski, P., Geng, Y., Ryder-Cook, A.S., Barnard, E.A., Darlison, M.G. and Barnard, P.J. (1989) The molecular basis of muscular dystrophy in the mdx mouse: a point mutation. *Science*, **244**, 1578–1580.
4. Gerhart, J., Bast, B., Neely, C., Iem, S., Amegbe, P., Niewenhuis, R., Miklasz, S., Cheng, P.F. and George-Weinstein, M. (2001) MyoD-positive myoblasts are present in mature fetal organs lacking skeletal muscle. *J. Cell Biol.*, **155**, 381–392.
5. Skuk, D., Goulet, M., Roy, B., Chapdelaine, P., Bouchard, J.P., Roy, R., Dugre, F.J., Sylvain, M., Lachance, J.G., Deschenes, L. *et al.* (2006) Dystrophin expression in muscles of Duchenne muscular dystrophy patients after high-density injections of normal myogenic cells. *J. Neuropathol. Exp. Neurol.*, **65**, 371–386.
6. Skuk, D., Goulet, M., Roy, B., Piette, V., Cote, C.H., Chapdelaine, P., Hogrel, J.Y., Paradis, M., Bouchard, J.P., Sylvain, M. *et al.* (2007) First test of a 'high-density injection' protocol for myogenic cell transplantation throughout large volumes of muscles in a Duchenne muscular dystrophy patient: eighteen months follow-up. *Neuromuscul. Disord.*, **17**, 38–46.
7. Dezawa, M., Ishikawa, H., Itokazu, Y., Yoshihara, T., Hoshino, M., Takeda, S., Ide, C. and Nabeshima, Y. (2005) Bone marrow stromal cells generate muscle cells and repair muscle degeneration. *Science*, **309**, 314–317.
8. De Bari, C., Dell'Accio, F., Vandenabeele, F., Vermeesch, J.R., Raymackers, J.M. and Luyten, F.P. (2003) Skeletal muscle repair by adult human mesenchymal stem cells from synovial membrane. *J. Cell Biol.*, **160**, 909–918.
9. Cui, C.H., Uyama, T., Miyado, K., Terai, M., Kyo, S., Kiyono, T. and Umezawa, A. (2007) Menstrual blood-derived cells confer human dystrophin expression in the murine model of Duchenne muscular dystrophy via cell fusion and myogenic transdifferentiation. *Mol. Biol. Cell*, **18**, 1586–1594.
10. Carosella, E.D., Paul, P., Moreau, P. and Rouas-Freiss, N. (2000) HLA-G and HLA-E: fundamental and pathophysiological aspects. *Immunol. Today*, **21**, 532–534.
11. Ulbrecht, M., Honka, T., Person, S., Johnson, J.P. and Weiss, E.H. (1992) The HLA-E gene encodes two differentially regulated transcripts and a cell surface protein. *J. Immunol.*, **149**, 2945–2953.
12. Braud, V.M., Allan, D.S., O'Callaghan, C.A., Soderstrom, K., D'Andrea, A., Ogg, G.S., Lazetic, S., Young, N.T., Bell, J.I., Phillips, J.H. *et al.* (1998) HLA-E binds to natural killer cell receptors CD94/NKG2A, B and C. *Nature*, **391**, 795–799.
13. Lee, N., Llano, M., Carretero, M., Ishitani, A., Navarro, F., Lopez-Botet, M. and Geraghty, D.E. (1998) HLA-E is a major ligand for the natural killer inhibitory receptor CD94/NKG2A. *Proc. Natl Acad. Sci. USA*, **95**, 5199–5204.
14. Borrego, F., Ulbrecht, M., Weiss, E.H., Coligan, J.E. and Brooks, A.G. (1998) Recognition of human histocompatibility leukocyte antigen (HLA)-E complexed with HLA class I signal sequence-derived peptides by CD94/NKG2 confers protection from natural killer cell-mediated lysis. *J. Exp. Med.*, **187**, 813–818.
15. Tsuji, H., Miyoshi, S., Ikegami, Y., Hida, N., Asada, H., Togashi, I., Suzuki, J., Satake, M., Nakamizo, H., Tanaka, M. *et al.* (2010) Xenografted human amniotic membrane-derived mesenchymal stem cells are immunologically tolerated and transdifferentiated into cardiomyocytes. *Circ. Res.*, **106**, 1613–1623.
16. Coupel, S., Moreau, A., Hamidou, M., Horejsi, V., Soulillou, J.P. and Charreau, B. (2007) Expression and release of soluble HLA-E is an immunoregulatory feature of endothelial cell activation. *Blood*, **109**, 2806–2814.
17. Faustman, D. and Coe, C. (1991) Prevention of xenograft rejection by masking donor HLA class I antigens. *Science*, **252**, 1700–1702.
18. Mendell, J.R., Kissel, J.T., Amato, A.A., King, W., Signore, L., Prior, T.W., Sahenk, Z., Benson, S., McAndrew, P.E., Rice, R. *et al.* (1995) Myoblast transfer in the treatment of Duchenne's muscular dystrophy. *N. Engl. J. Med.*, **333**, 832–838.
19. Mori, T., Kiyono, T., Imabayashi, H., Takeda, Y., Tsuchiya, K., Miyoshi, S., Makino, H., Matsumoto, K., Saito, H., Ogawa, S. *et al.* (2005) Combination of hTERT and bmi-1, E6, or E7 induces prolongation of the life span of bone marrow stromal cells from an elderly donor without affecting their neurogenic potential. *Mol. Cell. Biol.*, **25**, 5183–5195.
20. Li, J., Goldstein, I., Glickman-Nir, E., Jiang, H. and Chess, L. (2001) Induction of TCR Vbeta-specific CD8+ CTLs by TCR Vbeta-derived peptides bound to HLA-E. *J. Immunol.*, **167**, 3800–3808.
21. Hu, D., Ikizawa, K., Lu, L., Sanchirico, M.E., Shinohara, M.L. and Cantor, H. (2004) Analysis of regulatory CD8 T cells in Qa-1-deficient mice. *Nat. Immunol.*, **5**, 516–523.
22. Bryan, B.A., Walshe, T.E., Mitchell, D.C., Havumaki, J.S., Saint-Geniez, M., Maharaj, A.S., Maldonado, A.E. and D'Amore, P.A. (2008) Coordinated vascular endothelial growth factor expression and signaling during skeletal myogenic differentiation. *Mol. Biol. Cell*, **19**, 994–1006.
23. Darabi, R., Gehlbach, K., Bachoo, R.M., Kamath, S., Osawa, M., Kamm, K.E., Kyba, M. and Perlingeiro, R.C. (2008) Functional skeletal muscle regeneration from differentiating embryonic stem cells. *Nat. Med.*, **14**, 134–143.
24. Friedenstein, A.J., Gorskaja, J.F. and Kulagina, N.N. (1976) Fibroblast precursors in normal and irradiated mouse hematopoietic organs. *Exp. Hematol.*, **4**, 267–274.
25. Bieback, K., Kern, S., Kluter, H. and Eichler, H. (2004) Critical parameters for the isolation of mesenchymal stem cells from umbilical cord blood. *Stem Cells*, **22**, 625–634.
26. In 't Anker, P.S., Scherjon, S.A., Kleijburg-van der Keur, C., de Groot-Swings, G.M., Claas, F.H., Fibbe, W.E. and Kanhai, H.H. (2004) Isolation of mesenchymal stem cells of fetal or maternal origin from human placenta. *Stem Cells*, **22**, 1338–1345.
27. In 't Anker, P.S., Scherjon, S.A., Kleijburg-van der Keur, C., Noort, W.A., Claas, F.H., Willemze, R., Fibbe, W.E. and Kanhai, H.H. (2003) Amniotic fluid as a novel source of mesenchymal stem cells for therapeutic transplantation. *Blood*, **102**, 1548–1549.
28. Prockop, D.J. (1997) Marrow stromal cells as stem cells for nonhematopoietic tissues. *Science*, **276**, 71–74.
29. Kohyama, J., Abe, H., Shimazaki, T., Koizumi, A., Nakashima, K., Gojo, S., Taga, T., Okano, H., Hata, J. and Umezawa, A. (2001) Brain from bone: efficient 'meta-differentiation' of marrow stroma-derived mature osteoblasts to neurons with Noggin or a demethylating agent. *Differentiation*, **68**, 235–244.
30. Horwitz, E.M., Gordon, P.L., Koo, W.K., Marx, J.C., Neel, M.D., McNall, R.Y., Muul, L. and Hofmann, T. (2002) Isolated allogeneic bone marrow-derived mesenchymal cells engraft and stimulate growth in children with osteogenesis imperfecta: implications for cell therapy of bone. *Proc. Natl Acad. Sci. USA*, **99**, 8932–8937.
31. Miyoshi, H., Takahashi, M., Gage, F.H. and Verma, I.M. (1997) Stable and efficient gene transfer into the retina using an HIV-based lentiviral vector. *Proc. Natl Acad. Sci. USA*, **94**, 10319–10323.

Differential effect of statins on diabetic nephropathy in db/db mice

YUKINORI TAMURA[1,3], TOSHINORI MURAYAMA[1], MANABU MINAMI[1], MASAYUKI YOKODE[1] and HIDENORI ARAI[2]

Departments of [1]Clinical Innovative Medicine and [2]Human Health Sciences, Kyoto University Graduate School of Medicine, Shogoin, Sakyo-ku, Kyoto 606-8507, Japan

Received June 3, 2011; Accepted July 6, 2011

DOI: 10.3892/ijmm.2011.769

Abstract. Recent studies suggest a potential benefit of the lipid-lowering medication in the treatment of chronic kidney disease (CKD) such as diabetic nephropathy. Although statins have been widely used to lower serum cholesterol levels, the effect of these drugs on diabetic nephropathy has not been fully elucidated. In the present study, therefore, we addressed the role of different kinds of statins on diabetic nephropathy in db/db mice. Mice were fed with a standard diet with 0.005% (w/w) of pitavastatin, rosuvastatin, and pravastatin for 8 weeks starting from 8 weeks of age. The treatment with statins did not affect the food intake, body weight gain, adiposity, or blood pressure in db/db mice. Treatment with statins also had no effect on plasma lipid levels. In terms of the effect on albuminuria, pitavastatin and rosuvastatin reduced the urinary excretion of albumin by 60 and 40%, respectively, but not pravastatin, suggesting the effect of these two drugs on diabetic nephropathy. Furthermore, pitavastatin and rosuvastatin improved glomerular hypertrophy. All statins treatment improved insulin resistance. In addition, rosuvastatin and pravastatin treatment reduced oxidative stress measured by urinary 8-OHdG level, whereas the statins had no effect on the inflammatory response in the kidney of db/db mice. These results are not consistent with the renoprotective effect of statins. In conclusion, our data suggest that pitavastatin and rosuvastatin can improve diabetic nephropathy through the suppression of glomerular hypertrophy, independent of lipid-lowering or anti-oxidative effects.

Introduction

Diabetic nephropathy is one of the most common forms of chronic kidney disease (CKD) and the most frequent cause of mortality in patients with diabetes (1,2). The number of people affected by diabetic nephropathy or who need renal replacement is steadily increasing (3). Therefore, the establishment of therapeutic strategies for diabetic nephropathy is needed. Diabetic nephropathy results from complex interactions between genetic, metabolic, and hemodynamic factors, and can be characterized by mesangial expansion followed by glomerulosclerosis and a decline in renal function. The development of glomerulosclerosis in diabetes mellitus is always preceded by persistent albuminuria and glomerular hypertrophy (2). Therefore, these two manifestations could be promising therapeutic targets for the treatment of diabetic nephropathy.

3-Hydroxy-3-methylglutaryl (HMG)-coenzyme A (CoA) reductase inhibitors (statins) are widely used for diabetic patients to reduce their cardiovascular risk (4). Statins also have renoprotective actions and have been shown to reduce albuminuria in both experimental and clinical diabetic renal disease (5-8). Some of these benefits may be due to lipid lowering, since lipid levels are strongly associated with the development and progression of diabetic kidney disease (9,10). On the other hand, statins have a range of lipid-independent actions on cell proliferation, inflammation, and oxidative stress (11,12), which may impact the development and progression of renal damage in diabetes. These pleiotropic effects have been suggested to contribute to the renoprotective effect of statins. However, the precise mechanisms of the renoprotective effects are not fully understood. In addition, whether different statins have the same effect on diabetic nephropathy is not well known.

In this study, we addressed the role of various statins, such as pitavastatin, rosuvastatin, and pravastatin on the development of diabetic nephropathy in db/db mice.

Materials and methods

Materials. Pravastatin and rosuvastatin were provided by Daiichi Sankyo Co., Ltd. and pitavastatin was provided by Kowa Pharmaceutical Co., Ltd.

Animal procedure and experimental design. Male db/db mice (n=24) and their lean control db/m (n=6) mice were obtained from Charles River at 6 weeks of age. The mice were fed with normal chow without additional supplementation (non-treated group) or with chow supplemented with 0.005% (w/w) pravastatin, pitavastatin or rosuvastatin for 8 weeks starting from 8

Correspondence to: Dr Hidenori Arai, Department of Human Health Sciences, Kyoto University Graduate School of Medicine, 53 Kawahara-cho, Shogoin, Sakyo-ku, Kyoto 606-8507, Japan
E-mail: harai@kuhp.kyoto-u.ac.jp

Present address: [3]Department of Physiology and Regenerative Medicine, Kinki University School of Medicine, 377-2 Ohno-higashi, Osakasayama, Osaka 589-8551, Japan

Key words: statin, diabetic nephropathy, albuminuria, pleiotropic action

Table I. Characteristics of db/m and db/db mice treated with or without statins.

		db/db			
	db/m	Con	Pra	Pit	Ros
Body weight (g)	32.5±0.40	53.1±3.90	51.2±5.1	50.3±3.80	51.3±5.70
Liver weight (g)	1.15±0.29	2.99±0.41	2.78±0.54	2.55±0.36	3.19±0.85
eWAT weight (g)	0.37±0.05	3.23±0.25	3.08±0.59	3.01±0.41	3.10±0.62
Kidney weight (g)	0.31±0.07	0.50±0.02	0.51±0.06	0.42±0.01[a]	0.41±0.03[a]
Food intake (g/day)	3.82±0.33	7.45±2.43	7.15±0.72	7.70±1.65	7.04±1.58
SBP (mmHg)	NA	113.2±11.6	113.5±3.00	109.5±9.50	114.6±5.60

Con, control; Pra, pravastatin; Pit, pitavastatin; Ros, rosuvastatin; eWAT, epididymal white adipose tissue; SBP, systolic blood pressure. Results are expressed as mean ± SD (n=6 in each group). [a]P<0.05 vs. Con.

weeks of age. Animals had access to food and water *ad libitum* and were maintained on a 12-h light/dark cycle. All animal experiments were conducted according to the Guidelines for Animal Experiments at Kyoto University.

Analysis of metabolic parameter. Plasma glucose concentration was measured with a Glutest Ace (Sanwa Kagaku Kenkyusho Co., Ltd.). Plasma insulin concentration was measured with an insulin assay kit (Morinaga Institute of Biological Science). Plasma cholesterol and triglyceride levels were respectively measured with the Cholesterol E and Triglyceride E tests (Wako Pure Chemical Industries, Ltd.).

Measurement of urinary albumin and creatinine. Urinary albumin and creatinine were measured at 16 weeks of age from 24-h collection samples from mice housed in individual metabolic cages. During the urine collection, the mice were allowed free access to food and water. Albumin concentration in the urine was measured by Albuwell (Exocell). Urinary creatinine was measured with a Hitachi Mode 736 analyzer (Hitachi). The urinary albumin concentration was adjusted by the urinary creatinine concentration.

Measurement of urinary oxidative stress. Urinary 8-OHdG concentrations were measured at 16 weeks of age using a competitive enzyme-linked immunosorbent assay kit (8-OHdG Check, Japan Institute for the Control of Aging). Urinary 8-OHdG excretion was expressed as the total amount excreted in 24 h.

Quantitative real-time PCR. Total-RNA was extracted from frozen kidney tissue (50 mg) at 16 weeks of age using an RNeasy mini kit (Qiagen). The cDNA was synthesized from total-RNA using SuperScript III (Invitrogen). Real-time PCR was performed on an ABI PRISM 7900 using the SYBR-Green PCR Master Mix (Applied Biosystems). Primer sets were as follows: tumor necrosis factor (TNF)-α forward, 5'-CCCAGA CCCTCACACTCAGATC-3' and reverse, 5'-GCCACTCCAG CTGCTCCTC-3'; β-actin forward, 5'-TACCACAGGCATTG TGATGG-3' and reverse, 5'-TTTGATGTCACGCACGAT TT-3'. The mRNA levels were normalized relative to the amount of β-actin mRNA and expressed in arbitrary units.

Measurement of glomerular size. The mice were euthanized at 16 weeks of age. The kidneys were rapidly fixed in 10% formaldehyde, and embedded in paraffin. Paraffin sections were cut at 3 μm. For measurement of the glomerular size, paraffin sections were stained with hematoxylin and eosin. The size of the glomerular surface area was measured using the Image-Pro Plus software version 3.0.1 (Media Cybernetics, Inc.).

Statistical analysis. Data are expressed as the mean ± SD. Multiple comparisons among the groups were conducted by one-way analysis of variance with Fisher's PLSD test for post hoc analysis. P-values of <0.05 were considered significant.

Results

Effect of statin treatment on body weight, adiposity and systolic blood pressure. In db/db mice fed with a standard diet for 8 weeks starting at 8 weeks of age, body weight, epididymal white adipose tissue (eWAT) weight, liver weight were increased compared to those of db/m mice. Treatment with statins had no effect on body weight, food intake, liver weight and eWAT weight in db/db mice (Table I). In addition, there was no difference in systolic blood pressure between statin-treated and non-treated db/db mice.

Effect of statin treatment on renal function in db/db mice. Because albuminuria reflects renal function (13), we measured the urinary excretion of albumin in normal chow-fed db/db mice at 16 weeks of age. Urinary excretion of albumin was markedly increased in db/db mice compared with db/m mice (Fig. 1). Pitavastatin, rosuvastatin, but not pravastatin improved albuminuria in db/db mice. Kidney weights in pitavastatin- and rosuvastatin-treated db/db mice were reduced compared with non-treated db/db mice (Table I). These data suggest that pitavastatin and rosuvastatin treatment improves renal function in db/db mice.

Effect of statin treatment on plasma lipid level in db/db mice. To clarify the mechanism by which statins ameliorated renal function, we first examined the effect of statin treatment on lipid metabolism in db/db mice. Plasma triglyceride and total cholesterol level were increased in non-treated db/db mice compared with db/m mice (Fig. 2A and B). On the other hand,

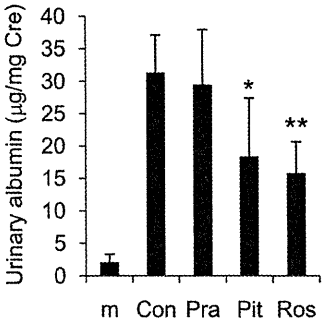

Figure 1. Effect of statins on renal function in db/db mice. The graph shows the urinary excretion of albumin in db/m mice (m), non-treated (Con), pravastatin-treated (Pra), pitavastatin-treated (Pit) and rosuvastatin-treated (Ros) db/db mice. Results are expressed as mean ± SD. *P<0.05, **P<0.01 vs. non-treated db/db mice (n=6 in each group).

statin treatment had no effect on plasma lipid levels in db/db mice (Fig. 2A and B), suggesting that the renoprotective effect of statins is independent of their lipid-lowering action.

Effect of statin treatment on insulin resistance in db/db mice. It has been reported that the development of insulin resistance contributes to renal dysfunction (14). Therefore, we next examined the effect of statin treatment on glucose metabolism in db/db mice. Blood glucose level, plasma insulin level, and HOMA-IR were markedly increased in db/db mice compared with db/m mice, indicating an increase in insulin resistance (Fig. 2C-E). Although statin treatment had no effect on plasma glucose, all statins reduced plasma insulin levels, resulting in a decrease in HOMA-IR (Fig. 2C-E). The data suggest that statin treatment improves insulin resistance.

Because hypoadiponectinemia is associated with the development of insulin resistance and kidney disease (15), we examined the effect of statin treatment on plasma adiponectin levels in db/db mice. In non-treated db/db mice, plasma adiponectin levels were decreased compared with db/m mice. Meanwhile, statin treatment had no effect on plasma adiponectin level in db/db mice (Fig. 2F).

Effect of statin treatment on the renal inflammation in db/db mice. Accumulating evidence now indicates that inflammatory mechanisms play a significant role in the development and progression of diabetic nephropathy. Especially, TNF-α is a pleiotropic inflammatory cytokine and has been shown to cause enhanced albumin permeability (16). Therefore, we next examined the effect of statin treatment on inflammation in the kidney of db/db mice. The expression of TNF-α mRNA was increased in the kidney of db/db mice compared with that of db/m mice, whereas statin treatment had no effect on its expression in db/db mice (Fig. 3A). These data suggest that statins had no effect on the inflammatory response in the kidneys of db/db mice.

Effect of statin treatment on the oxidative stress in db/db mice. To examine the effect of statin treatment on oxidative stress, we measured urinary 8-OHdG concentrations in db/db mice. Urinary 8-OHdG levels in non-treated db/db mice were significantly higher than those in db/m mice. Pravastatin and rosuvastatin reduced urinary 8-OHdG levels in db/db mice, whereas pitavastatin had no effect on oxidative stress despite detecting the amelioration of albuminuria (Fig. 3B).

Effect of statin treatment on glomerular hypertrophy in db/db mice. Glomerular hypertrophy is a hallmark in diabetic

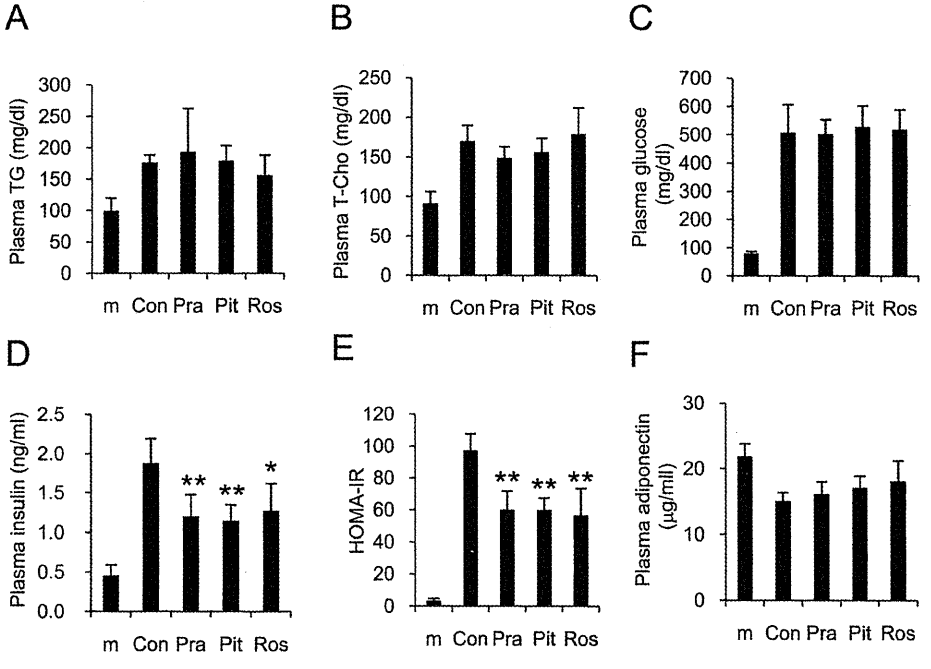

Figure 2. Effect of statins on lipid and glucose metabolism in db/db mice. (A) Plasma triglyceride (TG), (B) total cholesterol (T-Cho), (C) glucose, (D) insulin, (E) HOMA-IR and (F) adiponectin levels in db/m mice (m), non-treated (Con), pravastatin-treated (Pra), pitavastatin-treated (Pit) and rosuvastatin-treated (Ros) db/db mice. Results are expressed as mean ± SD. *P<0.05, **P<0.01 vs. non-treated db/db mice (n=6 in each group).

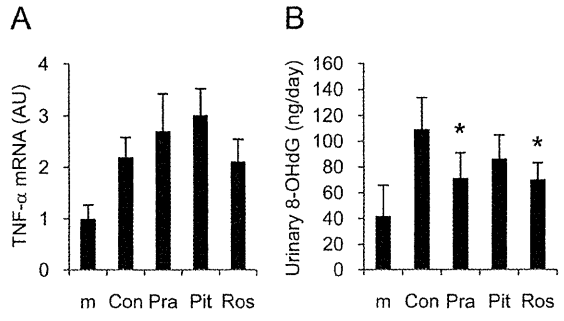

Figure 3. Effect of statins on renal inflammation and oxidative stress in db/db mice. (A) Expression of TNF-α mRNA in whole kidney and (B) urinary 8-OHdG levels in db/m mice (m), non-treated (Con), pravastatin-treated (Pra), pitavastatin-treated (Pit) and rosuvastatin-treated (Ros) db/db mice. Results are expressed as mean ± SD. *P<0.05 vs. non-treated db/db mice (n=6 in each group).

nephropathy along with albuminuria. Therefore, we assessed the glomerular hypertrophy in db/db mice and the effect of statins by measuring the glomerular surface area. Mean glomerular surface area size in db/db mice was increased compared with db/m mice. Pitavastatin and rosuvastatin treatment, but not pravastatin treatment, suppressed the glomerular hypertrophy as well as urinary excretion of albumin in db/db mice (Fig. 4).

Discussion

In the present study, we showed that pitavastatin and rosuvastatin treatment improved albuminuria and suppressed glomerular hypertrophy, independent of its lipid-lowering and anti-oxidative effect in db/db mice.

In CKD patients, there is an increase in total cholesterol and LDL levels (17). The level of cholesterol is directly correlated with the degree of albuminuria (18), suggesting that hyperlipidemia is associated with the development of CKD such as diabetic nephropathy. In fact, lipid-lowering therapy by statin has been successful to the amelioration of renal function in patients with diabetic nephropathy (19,20). However, the present study and other animal studies showed that statin treatment significantly improved renal function without affecting the plasma lipid profile (5,8,21). Therefore, the renoprotective effect of statins may be mainly caused by its pleiotropic action rather than their lipid-lowering action.

Insulin resistance is associated with the development of renal dysfunction in type 2 diabetes. It has been shown that insulin resistance correlates with the onset of microalbuminuria in patients with type 2 diabetes as well as in nondiabetic subjects (14). Several studies showed that amelioration of insulin resistance resulted in a restoration of renal function (22-24). Statin also has an ability to ameliorate insulin resistance. Takagi *et al* (25) reported that pravastatin treatment improved insulin resistance through the increase in plasma adiponectin levels in db/db mice. In the present study, we also observed that all statin treatment improved insulin resistance detected by the reduction of HOMA-IR, while adiponectin was not altered by statin treatment in db/db mice. However, this amelioration was not consistent with the renoprotective effects of statins in db/db mice.

Oxidative stress and inflammation are also far more prevalent in CKD patients than in normal subjects (26). In the present study, we also observed the elevation of oxidative stress and inflammation in the kidneys of db/db mice compared with that of lean control mice. Renal disease is associated with a graded increase in oxidative stress markers even in early CKD (27). This oxidative stress can accelerate renal injury progression. In addition, inflammatory markers such as C reactive protein and cytokines increase with renal function deterioration suggesting that CKD is a low-grade inflammatory process (28). Therefore, the agents which have anti-oxidative and anti-inflammatory action have been attracted as a therapeutic strategy for renal dysfunction (29). Anti-oxidative and anti-inflammatory actions are also major pleiotropic effects of statins (12). Several reports have shown that these actions of statins contribute to their renoprotective effects (5,30,31). In the present study, we also observed that pravastatin and rosuvastatin suppressed oxidative stress in db/db mice as well as these reports, whereas we could not detect the anti-inflammatory effect of statins in the kidneys of db/db mice. Pitavastatin had no effect on oxidative stress, despite the presence of the restored renal function in db/db mice. This result suggests that the anti-oxidant action of statins is not primarily responsible for their renoprotective effect.

In the present study, we observed a correlation between the renoprotective effects of statins and their suppressive effect

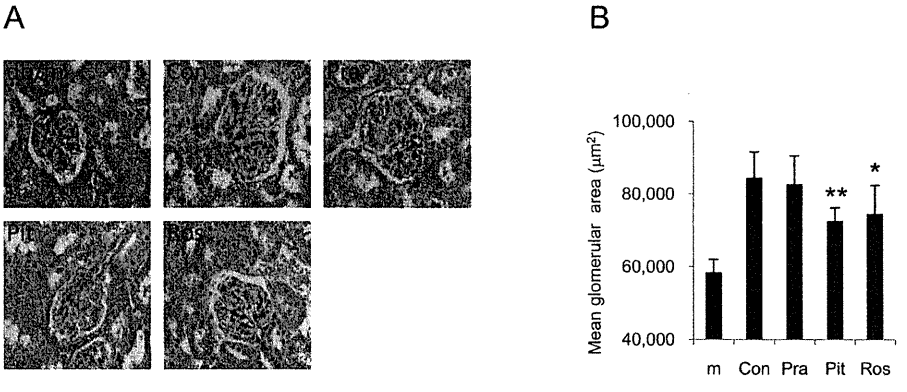

Figure 4. Effects of statins on the glomerular hypertrophy in db/db mice. (A) H&E staining of glomeruli (magnification, x200) and (B) mean glomerular surface area of db/m mice (m), non-treated (Con), pravastatin-treated (Pra), pitavastatin-treated (Pit) and rosuvastatin-treated (Ros) db/db mice. The mean area of fifty glomeruli per mouse was analyzed. Results are expressed as mean ± SD. *P<0.05, **P<0.01 vs. non-treated db/db mice (n=6 in each group).

of glomerular hypertrophy in db/db mice. The glomerular morphological changes in diabetic nephropathy are characterized primarily by mesangial expansion and glomerular based membrane (GBM) thickening. It has been reported that the dysregulated cell cycle by the increased inhibitor of cyclin dependent kinase (such as p21 and p27) contributes to these morphological changes and renal dysfunction (32,33). Pleiotropic effects of statins on the cell cycle are well known (12). Furthermore, Danesh *et al* (34) reported that statin treatment normalized the cell cycle through the suppression of p21 expression in high glucose-stimulated mesangial cells. In the present study, pleiotropic effects of statin on the cell cycle thus might improve glomerular hypertrophy and albuminuria. However, further study is required to clarify the effect of statins in glomerular hypertrophy and renal dysfunction.

In conclusion, we have shown the effects of various statins on diabetic nephropathy in db/db mice. Our study suggests that its renoprotective effect is mainly dependent on suppressing the glomerular hypertrophy, independent of its lipid-lowering or anti-oxidative effects, and there may be differences in the renoprotective ability between various statins.

Acknowledgements

We thank Dr Takeshi Matsubara (Kyoto University) for helpful discussion and critical reading of our manuscript. We also thank Nami Sawada (Kyoto University) for excellent technical assistance. This study was supported by the Takeda Science Foundation.

References

1. Mauer SM, Steffes MW, Ellis EN, Sutherland DE, Brown DM and Goetz FC: Structural-functional relationships in diabetic nephropathy. J Clin Invest 74: 1143-1155, 1984.
2. Nagai K, Arai H, Yanagita M, *et al*: Growth arrest-specific gene 6 is involved in glomerular hypertrophy in the early stage of diabetic nephropathy. J Biol Chem 278: 18229-18234, 2003.
3. Coresh J, Selvin E, Stevens LA, *et al*: Prevalence of chronic kidney disease in the United States. JAMA 298: 2038-2047, 2007.
4. Athyros VG, Mitsiou EK, Tziomalos K, Karagiannis A and Mikhailidis DP: Impact of managing atherogenic dyslipidemia on cardiovascular outcome across different stages of diabetic nephropathy. Expert Opin Pharmacother 11: 723-730, 2010.
5. Fujii M, Inoguchi T, Maeda Y, *et al*: Pitavastatin ameliorates albuminuria and renal mesangial expansion by downregulating NOX4 in db/db mice. Kidney Int 72: 473-480, 2007.
6. Kolavennu V, Zeng L, Peng H, Wang Y and Danesh FR: Targeting of RhoA/ROCK signaling ameliorates progression of diabetic nephropathy independent of glucose control. Diabetes 57: 714-723, 2008.
7. Nakamura T, Ushiyama C, Hirokawa K, Osada S, Shimada N and Koide H: Effect of cerivastatin on urinary albumin excretion and plasma endothelin-1 concentrations in type 2 diabetes patients with microalbuminuria and dyslipidemia. Am J Nephrol 21: 449-454, 2001.
8. Ota T, Takamura T, Ando H, Nohara E, Yamashita H and Kobayashi K: Preventive effect of cerivastatin on diabetic nephropathy through suppression of glomerular macrophage recruitment in a rat model. Diabetologia 46: 843-851, 2003.
9. Rosario RF and Prabhakar S: Lipids and diabetic nephropathy. Curr Diab Rep 6: 455-462, 2006.
10. Thomas MC, Rosengard-Barlund M, Mills V, *et al*: Serum lipids and the progression of nephropathy in type 1 diabetes. Diabetes Care 29: 317-322, 2006.
11. Campus G, Salem A, Sacco G, Maida C, Cagetti MG and Tonolo G: Clinical effects of mechanical periodontal therapy in type 2 diabetic patients. Diabetes Res Clin Pract 75: 368-369, 2007.
12. Haslinger-Loffler B: Multiple effects of HMG-CoA reductase inhibitors (statins) besides their lipid-lowering function. Kidney Int 74: 553-555, 2008.
13. Dronavalli S, Duka I and Bakris GL: The pathogenesis of diabetic nephropathy. Nat Clin Pract Endocrinol Metab 4: 444-452, 2008.
14. Jauregui A, Mintz DH, Mundel P and Fornoni A: Role of altered insulin signaling pathways in the pathogenesis of podocyte malfunction and microalbuminuria. Curr Opin Nephrol Hypertens 18: 539-545, 2009.
15. Tesauro M, Canale MP, Rodia G, *et al*: Metabolic syndrome, chronic kidney, and cardiovascular diseases: role of adipokines. Cardiol Res Pract 2011: 653182, 2011.
16. Navarro-Gonzalez JF and Mora-Fernandez C: The role of inflammatory cytokines in diabetic nephropathy. J Am Soc Nephrol 19: 433-442, 2008.
17. Kwan BC, Beddhu S, Kronenberg F and Cheung AK: Does statin therapy improve cardiovascular outcomes in patients with type 2 diabetes receiving hemodialysis? Nat Clin Pract Nephrol 2: 76-77, 2006.
18. Kaysen GA, Gambertoglio J, Felts J and Hutchison FN: Albumin synthesis, albuminuria and hyperlipemia in nephrotic patients. Kidney Int 31: 1368-1376, 1987.
19. Tonolo G, Velussi M, Brocco E, *et al*: Simvastatin maintains steady patterns of GFR and improves AER and expression of slit diaphragm proteins in type II diabetes. Kidney Int 70: 177-186, 2006.
20. Sharp Collaborative Group: Study of Heart and Renal Protection (SHARP): randomized trial to assess the effects of lowering low-density lipoprotein cholesterol among 9,438 patients with chronic kidney disease. Am Heart J 160: 785-794 e10, 2010.
21. Usui H, Shikata K, Matsuda M, *et al*: HMG-CoA reductase inhibitor ameliorates diabetic nephropathy by its pleiotropic effects in rats. Nephrol Dial Transplant 18: 265-272, 2003.
22. Okada T, Wada J, Hida K, *et al*: Thiazolidinediones ameliorate diabetic nephropathy via cell cycle-dependent mechanisms. Diabetes 55: 1666-1677, 2006.
23. Baylis C, Atzpodien EA, Freshour G and Engels K: Peroxisome proliferator-activated receptor [gamma] agonist provides superior renal protection versus angiotensin-converting enzyme inhibition in a rat model of type 2 diabetes with obesity. J Pharmacol Exp Ther 307: 854-860, 2003.
24. Miyazaki Y, Cersosimo E, Triplitt C and DeFronzo RA: Rosiglitazone decreases albuminuria in type 2 diabetic patients. Kidney Int 72: 1367-1373, 2007.
25. Takagi T, Matsuda M, Abe M, *et al*: Effect of pravastatin on the development of diabetes and adiponectin production. Atherosclerosis 196: 114-121, 2008.
26. Schiffrin EL, Lipman ML and Mann JF: Chronic kidney disease: effects on the cardiovascular system. Circulation 116: 85-97, 2007.
27. Krane V and Wanner C: The metabolic burden of diabetes and dyslipidaemia in chronic kidney disease. Nephrol Dial Transplant 17 (Suppl 11): S23-S27, 2002.
28. Mora C and Navarro JF: Inflammation and diabetic nephropathy. Curr Diab Rep 6: 463-468, 2006.
29. Locatelli F, Canaud B, Eckardt KU, Stenvinkel P, Wanner C and Zoccali C: Oxidative stress in end-stage renal disease: an emerging threat to patient outcome. Nephrol Dial Transplant 18: 1272-1280, 2003.
30. Zhou MS, Schuman IH, Jaimes EA and Raij L: Renoprotection by statins is linked to a decrease in renal oxidative stress, TGF-beta, and fibronectin with concomitant increase in nitric oxide bioavailability. Am J Physiol Renal Physiol 295: F53-59, 2008.
31. Diepeveen SH, Verhoeven GW, Van Der Palen J, *et al*: Effects of atorvastatin and vitamin E on lipoproteins and oxidative stress in dialysis patients: a randomised-controlled trial. J Intern Med 257: 438-445, 2005.
32. Al-Douahji M, Brugarolas J, Brown PA, Stehman-Breen CO, Alpers CE and Shankland SJ: The cyclin kinase inhibitor p21WAF1/CIP1 is required for glomerular hypertrophy in experimental diabetic nephropathy. Kidney Int 56: 1691-1699, 1999.
33. Awazu M, Omori S, Ishikura K, Hida M and Fujita H: The lack of cyclin kinase inhibitor p27(Kip1) ameliorates progression of diabetic nephropathy. J Am Soc Nephrol 14: 699-708, 2003.
34. Danesh FR, Sadeghi MM, Amro N, *et al*: 3-Hydroxy-3-methylglutaryl CoA reductase inhibitors prevent high glucose-induced proliferation of mesangial cells via modulation of Rho GTPase/p21 signaling pathway: implications for diabetic nephropathy. Proc Natl Acad Sci USA 99: 8301-8305, 2002.